Synthesis and Characterization of Synthetic and Biopolymer Hydrogels

by

Marius Lilletveit

Faculty of Mathematics and Natural sciences

University of Bergen

August 2019

Acknowledgements

Completing this thesis, and with that my master's degree in chemistry at the University of Bergen, represents a major achievement in my life. First and foremost, I would like to thank my supervisor, Kristine Spildo, for her patience, encouragement, and support throughout the work of this thesis. A special thanks to Malgorzata Anna Wisniewska for providing me with this interesting subject, for valuable guidance, and for always taking the time to answer my many questions. I would also like to thank my friend Bakary Konateh for his good company and helpful advice. Last, but not least, I would like to express my gratitude to my girlfriend Irene and my parents, who have provided me with constant encouragement and motivation.

Abstract

Hydrogels are widely researched for biomedical applications such as drug delivery. The tunable properties of hydrogels, in terms of swelling, mechanical properties and mesh size, make them prime candidates for this application. Synthetic polymers display superior mechanical properties and swelling ability, but their toxicity, and lack of biodegradability and biocompatibility is problematic. Biopolymer hydrogels synthesized with either reduced, or without toxic crosslinker agents, could provide viable alternatives for biomedical applications.

This study details the approaches for synthesis of three main hydrogel formulations. The hydrogels were characterized by oscillatory rheological measurements, dynamic swelling, and pulsed gradient spin-echo NMR.

Poly(NIPAM-co-AAc) was synthesized by free radical polymerization, using a the redox couple (APS/TEMED) as initiators, and DAT as crosslinker. The hydrogel displayed good mechanical properties. Mass swelling ratio was shown to be greatly influenced by initiator ratio.

Self-assembling chitosan (SA-CS) hydrogel was prepared under mild reaction conditions. Crosslinking by Michael addition was performed by mixing of maleimide-modified and thiolated chitosan. Inconclusive results indicated the formation a weak reversible network, as well as a covalently crosslinked network with satisfactory swelling ability and mechanical properties.

Chitosan-gelatin hydrogel was dissolved in acetic acid and co-crosslinked by glutaraldehyde and sodium sulfate. Oscillatory rheological measurements indicated a trend between increasing amount of sodium sulfate and decreasing storage modulus. Dissolution in aqueous media and lack of swelling suggests it is an inadequate alternative to poly(NIPAM-co-AAc).

Table of contents

1 Introduction

Hydrogels are of great interest in pharmaceutical and medical industries due to their incredibly wide spectre of properties and applications. Essentially, any hydrophilic polymer can be used to form hydrogels, resulting in a huge variety of hydrogel's chemical composition and physical properties. Such properties include pH and temperature sensitivity, adhesiveness, and biocompatibility [1, 2]. Furthermore, properties such as mechanical strength, swelling degree, density of networks, and mesh size can be tuned. This facilitates the option of adapting hydrogel systems, increasing the efficiency within their area of use. Such areas can be drug delivery, tissue engineering and wound healing [3-5].

Poly(NIPAM-co-AAc) is a synthetic hydrogel which is pH and temperature sensitive. It exhibits excellent mechanical properties, and tunable swelling characteristics [1, 6, 7]. This makes poly(NIPAM-co-AAc) hydrogel a compelling candidate for tissue engineering and drug delivery [4, 8]. Despite these excellent properties, poly(NIPAM-co-AAc) is toxic and is not biocompatible [9]. For biomedical applications, hydrogels formulated from natural biopolymers could be better alternatives. Biopolymers such as chitosan and gelatin are biocompatible, biodegradable and non-toxic [10-12].

The aim of the present study is to investigate and compare the mechanical properties, swelling ability and microstructure of poly(NIPAM-co-AAc) hydrogel, with more biocompatible hydrogel formulations of chitosan and gelatin. The biopolymer hydrogels will be covalently crosslinked to increase mechanical properties. To reduce toxicity, biopolymer hydrogels will be crosslinked through either co-crosslinking, or polymer-polymer conjugation.

2 Background

2.1 Hydrogels

Hydrogels are three-dimensional, cross-linked, hydrophilic polymeric networks that can absorb and retain large amounts of water or biological fluids within it structure [13]. Their affinity to absorb water is due to the presence of hydrophilic groups, such as -OH-, -CONH-, -$CONH_2$-, and -SO_3H-, in the polymers that form the hydrogel network [9, 13]. This network contains critical crosslinks that are either physical or chemical. The crosslinks stem from covalent bonds, hydrogen bonding, van der Waals interactions or physical entanglements. Due to the presence of the crosslinks, rather than dissolving in the aqueous surroundings, hydrogels exhibit a swelling behaviour, see Hamidi [9] and the references cited therein. When in a swollen state, some of the hydrogels physical attributes are common to living tissue, such as low interfacial tension with water and biological fluids, and a soft rubbery consistency [9, 14].

They are generally non-toxic, biocompatible, and biodegradable. The biocompatibility of hydrogels stem from their large water content, as well as depending on the biocompatibility of the polymer of which they are formed [15]. The meaning of the word "biocompatibility" has been the subject of some discussion, and the definition may change based on context. In general, it can be defined as "the ability of a material to perform with an appropriate host response in a specific application" [16]. In simple terms it means that a biocompatible substance should be able to perform its desired function within a physiological environment without causing undesirable effects.

The physical form of the hydrogel can also be varied, as they may be formulated as films, microparticles, nanoparticles and coatings [5, 17, 18]. In terms of drug delivery, the ability to formulate hydrogels as nanoparticles is a big advantage. The nanoparticles provide targeted drug delivery, improved bioavailability, extended effect of the delivered drug or gene in target tissue, and increased stability of therapeutic agents against chemical and enzymatic degradation [9, 19, 20]

Due to the tunable physical and chemical properties of hydrogels, they are of great interest in medical and pharmaceutical industries. A large amount of research has been done to capitalize on these properties in the form of wound healing [5], biological tracing and delivery of genes [21], regenerative medicine [22], diagnostics [23], and drug delivery [24]. The use of hydrogels as drug delivery systems is an area that have gained a lot of scientific interest lately.

Due to the porous structure of hydrogels, it is possible to load the gel matrix with drug molecules [15]. The mechanisms of drug release from hydrogels can be categorized as: 1) diffusion-controlled, 2) swelling-controlled, and 3) chemically-controlled [9]. Following Fick's law of diffusion, the diffusion-controlled behaviour is the most applicable mechanism for describing drug release from hydrogels [9, 25]. The diffusion of drugs from hydrogels is mainly reliant on the mesh sizes within the hydrogel matrix, which can be described as the average distance between two adjacent crosslinks [9, 26]. The mesh size is mainly affected by the degree of crosslinking [15], and chemical structure of the composing monomers [9]. The drug diffusion coefficient decreases as the crosslinking density increases [26]. The physical properties of hydrogels, such as mechanical strength, degradability, and diffusivity are all partially controlled by the mesh size of the hydrogel network [9, 25-27].

One example of tuning hydrogel properties is by controlling the density of cross-links to affect this porous structure [15]. It has been shown that the degree of cross-links very much affects the diffusion coefficient of the drug molecule through the gel network [28]. As the crosslink density increases, the number of crosslinks per unit volume also increases, limiting the amount of free space in the network for accommodating water molecules. Furthermore, an increase in the rigidity of the network restricts the movement of macromolecular chains, leading to a lower degree of swelling [28].

To avoid surgery after drug release, it is important that hydrogels injected into the human body are biodegradable. Intelligent dissolution of hydrogels can be constructed through environmental pathways, such as pH and temperature [15]. Wu et.al designed a thermo-and-pH-sensitive hydrogel system where the dissolution of the hydrogel and subsequent drug release depended on surrounding pH values [29].

2.2 Classification of hydrogels

Hydrogels can be classified based on composition, cross-linking, physical structure, origin, and ionic charge [30]. Ross-Murphy and Simon [31] divides polymer gels into three classes; covalently cross-linked materials, entanglement networks, and physical gels. In the present study, we will treat the classification of hydrogels in a simplistic manner and divide them into two main categories; chemical/permanent gels and physical/reversible gels.

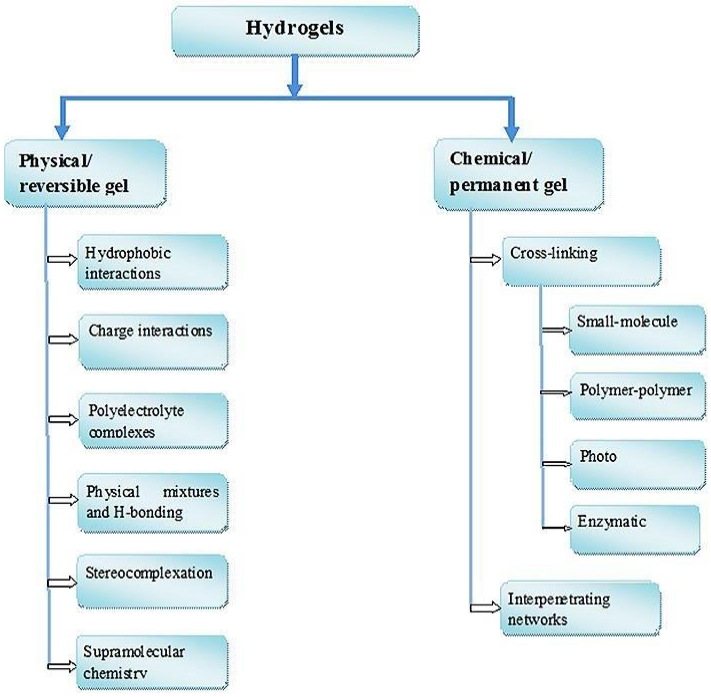

Figure 2.2: Classification of hydrogels. Illustration from Parhi [32]

2.2.1 Chemical/permanent hydrogel

Chemical crosslinking can be described as covalent interactions between polymer chains, resulting in junctions being formed in the polymeric network and a permanently crosslinked hydrogel. The covalent interactions are the main forces behind the hydrogel network formation. Nevertheless, secondary interactions such as hydrogen bonding and hydrophobic interactions also contributes to gel formation [33]. The permanent network allows for the absorption of water and bioactive compounds, and diffusion controlled drug release [15]. The formation of a permanent hydrogel network can be achieved by using small cross-linker molecules, polymer-polymer conjugation, photosensitive agents, or by enzyme catalysed reaction [32]. Only the first two methods are relevant for this thesis. The most common method of cross-linking is by using small cross-linker molecules that have at least two or more reactive functional groups, so that bridges between polymeric chains can be created [33]. However, the functional groups do not always react to form crosslinks. There is a possibility of intramolecular cyclization reactions, where both ends of the crosslinker molecule react into the same growing polymer chain, resulting in a loop structure [34]

Glutaraldehyde is commonly used to crosslink natural polymers such as chitosan and gelatine [24, 35, 36]. Dialdehydes react directly with amino groups in the polymer in aqueous media by forming covalent imine bonds via Schiff reaction, that are subsequently stabilized by resonance with adjacent ethylenic bonds [33, 37]. Dialdehydes, such as glutaraldehyde, have one main deficiency, they are generally considered toxic [38]. The biocompatibility of chemically crosslinked hydrogels is therefore reduced, as residual crosslinking molecules in the hydrogels may lead to unwanted and damaging effects.

A way of reducing the potential toxicity of permanent hydrogels is to use alternative crosslinking methods such as double crosslinking and polymer-polymer conjugation. Double crosslinking is a method where a non-toxic ionic crosslinker is used together with a standard crosslinker agent. In the case of glutaraldehyde, the ionic crosslinker sodium sulfate can be introduced to partially replace glutaraldehyde in the crosslinking of a hydrogel network [24].

Polymer-polymer conjugation is a method of achieving covalently cross-linked hydrogels without using cross-linker agents. A cross-linking reaction can occur between the structural units of two polymeric chains that are chemically different, with the prerequisite of reactive functional groups. Michael addition is a well-researched method of polymer-polymer conjugation in which cross-linking occurs through a nucleophilic addition of an amine or a thiol on a vinyl group [32].

Permanent hydrogels generally display good mechanical strength, they allow for absorption of aqueous media or biological fluids and exhibit great stability against degradation [15, 32].

2.2.2 Physical hydrogel

The gel network of physical hydrogels are relatively disordered [39], and are formed by various reversible links. Such links can be ionic interactions in the form of ionic crosslinking and polyelectrolyte complexes, or secondary interactions as in grafted hydrogels, entangled hydrogels, and chitosan/poly(vinyl alcohol) complexed hydrogels [33]. Hydrogels associated by such reversible links does not require covalent crosslinker molecules. The omittance of these potentially toxic molecules ensures that physical hydrogels can be safely used in clinical and medicinal applications. Although nontoxic, the effectiveness of physical hydrogels is an issue, as they have weak mechanical strength and dissolve in a manner that is hard to control [33].

2.3 Selected hydrogel systems

In this section the hydrogel systems that are studied in this thesis will be presented and discussed.

2.3.1 Poly(N-isopropylacrylamide-co-acrylic acid) hydrogel

Poly(N-isopropylacrylamide) (PNIPAAM) is a temperature responsive hydrogel that experience a thermoreversible phase separation at a lower critical solution temperature of 32°C. The phase separation occurs due to the interactions of polymer chains with water molecules being temperature dependent [1]. As a result, it is an interesting candidate for biomedical applications such as tissue engineering and drug delivery [4, 8]. The mechanical properties of PNIPAAM hydrogel is dependent on the swollen mesh size of the gel, which can be altered by the way the initiation of the hydrogel triggers the polymerization [40]. Denisin and Pruitt [7] studied polyacrylamide hydrogels crosslinked by bis-acrylamide. They found that polymerization time, polymerization temperature, and hydrogel formulation (total polymer concentration to crosslinker concentration ratio) affected the swelling behaviour of the gel, subsequently affecting gel structure and mechanical properties as the gel aged.

Poly(N-isopropylacrylamide-co-acrylic acid) [poly(NIPAM-co-AAc)] is a chemically synthesized copolymer hydrogel. The acrylic acid (AAc) is introduced as a co-monomer to keep the hydrogel from dissolving in water at low temperatures [41]. AAc is strongly hydrophilic and increases the volume phase transition temperature (VPTT) and water absorption ability of the hydrogel [42, 43]. Furthermore, AAc affects the conformational ordering of the hydrogel in some cases. This is exemplified with a decrease of hydrodynamic radius in the presence of electrolytes, and dissociation of AAc groups and corresponding hydrogel expansion in an increasing pH environment [6]. At higher pH, AAc was also shown to increase the transition temperature to approximately 55 °C, compared to 34 °C at low pH [6]. The weight percentage of AAc in poly(NIPAM-co-AAc) hydrogel have been proven to influence the pore size of the hydrogel [44].

Poly(acrylic acid), (PAAc), is a ionic polyelectrolyte, meaning that ionic interactions between the charged polymer and free ions contributes to the swelling of the hydrogel [13]. The carboxylic acid groups on the polymer chain facilitates the swelling ability of poly(acrylic acid). These groups are sensible to pH and ionic strength, meaning that the swelling ability of PAAc is affected by these factors [34].

Ammonium persulfate (APS) and N,N,N',N'-tetramethylethylenediamine (TEMED) is a redox couple that can be used to initiate the network formation reaction through a free radical copolymerization (FRC) [45]. The initiation is based on an autocatalytic reaction [46]. An autocatalytic reaction could accelerate the polymerization of the hydrogel network, leading to spatial fluctuations that result in regions of different polymer density in the network. Hydrogel networks formed through FRC are inhomogeneous due to the imbalance of reactive vinyl groups between crosslinker and monomer. At the beginning of polymerization, extensive crosslinking reactions occurs directly, yielding dense polymer regions. As polymerization continues, the crosslinking reaction is more gradual and less dense network domains are formed [40, 47].

Amount of initiator and the ratio between them has been shown to influence the gelation time of the hydrogel, and degree of swelling [40]. TEMED promotes the decomposition of APS into free radicals, thus accelerating polymerization and crosslinking [40, 48]. Compared to hydrogels derived from natural polymers, synthetic hydrogels are generally more toxic and less biocompatible. However, their mechanical properties are better, as well as exhibiting well defined and tunable degradation kinetics [9].

2.3.2 Self-assembling chitosan hydrogel

As mentioned in section 2.2.1, by using polymer-polymer conjugation, a permanent hydrogel with covalent crosslinking can be achieved without the use of crosslinker agent. Self-assembling chitosan (SA-CS) hydrogel is synthesized through Michael addition. The reaction scheme is presented in figure 2.3.2. The cationic chitosan polymer is modified with either thioglycolic acid or 4-maleimidobutyric acid, resulting in SH-CS and Mal-CS, respectively, through covalent bonds being created between the primary amino groups from chitosan and carboxylic acid groups. Gel formation occurs by mixing of the modified polymers through nucleophilic attack from the thiol in SH-CS on the vinyl group in Mal-CS [49].

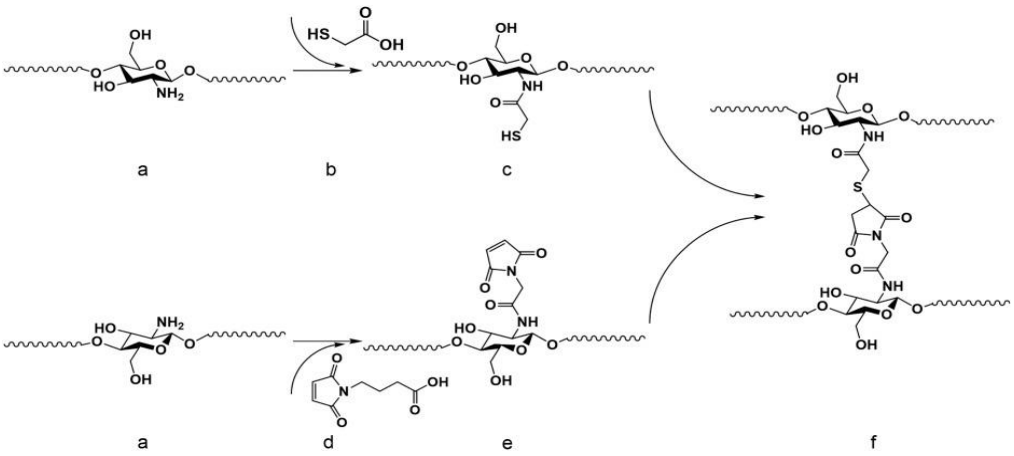

Figure 2.3.2: (a) Modification of CS (b) with either thioglycolic acid (c) resulting in SH-CS or (d) by the addition of 4-maleimidobutyric acid (e) leading to Mal-CS. Mixing aqueous solutions of the two polymers led to covalent crosslinking via (f) Michael addition and gelation [49]

Sa-CS hydrogel has been shown to have a porous structure, exhibiting the ability to swell in aqueous media and providing a sustained release of drugs. Despite the modification of polymers, SA-CS is biodegradable by lysozyme [49]. The modification of chitosan with thioglycolic acid also improve the hydrogels mucoadhesive properties, making it more favourable for oral drug delivery [50].

2.3.3 Chitosan hydrogel

Chitosan is prepared from deacetylation of chitin, which is an abundant natural polymer extracted from crustaceous shells, or some fungi [51, 52]. Chitosan contains a primary amino group and two hydroxyl groups for each C6 unit. The presence of free amino groups enhances the solubility and reactivity of chitosan with respect to chitin. The amino groups have a pKa value of approximately 6.5, which makes it soluble in weakly acidic solutions. At low pH values, the amino groups are protonated and become positively charged, making chitosan a water-soluble cationic polyelectrolyte [35, 51, 53]. When dissolved in acetic medium, entanglements is formed in the chitosan network, producing a weak physical hydrogel, see Berger [33] and references cited therein. The molecular weight and degree of deacetylation (DD) are the two main parameters that influence the properties of chitosan [54], affecting the antibacterial activity and biodegradation [55, 56].

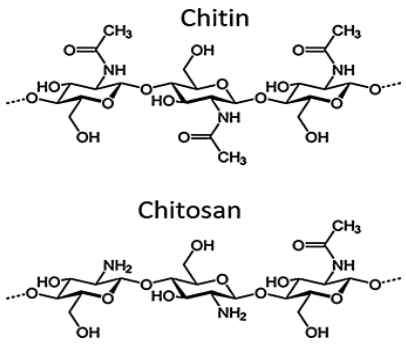

Figure 2.3.3: Chitin and chitosan [57]

There is a lot of attention on designing "intelligent" drug delivery systems (DDS) that can provide a controlled drug release. Hydrogels designed from natural polymers, such as chitosan, have been widely researched for this purpose. Chitosan is a promising candidate for drug delivery, due to its biodegradability, low toxicity, mucoadhesivity, promotion of wound healing, and bacteriostaticity [50, 56, 58, 59].

One of the most important facets of a DDS is biodegradation, the hydrogels metabolic fate in the body after drug release. The biodegradation of chitosan can be chemical, meaning acid catalysed degradation, or enzymatic [58]. Yang et.al [55] performed studies of in vivo and in vitro degradation of chitosan, finding that both rate and extent of degradation were strongly dependent on the degree of deacetylation, and increasing deacetylation decreased the degradation rate. Kean and Thanou [58] concluded that given sufficient time and appropriate conditions, it is likely that the degradation of chitosan is satisfactory for a DDS.

Chitosan can be applied for drug delivery, however, the release of solute from chitosan can be rapid and is not easily controllable [3]. The instability of chitosan can be solved, as the mechanical properties and degradation rate of chitosan is improved by introducing crosslinker molecules [22, 60]. To form a permanently crosslinked chitosan hydrogel, the polymer is often cross-linked by glutaraldehyde. Glutaraldehyde forms covalent imine bonds with the free amino groups of chitosan via Schiff reaction [2] (figure 2.3.4).

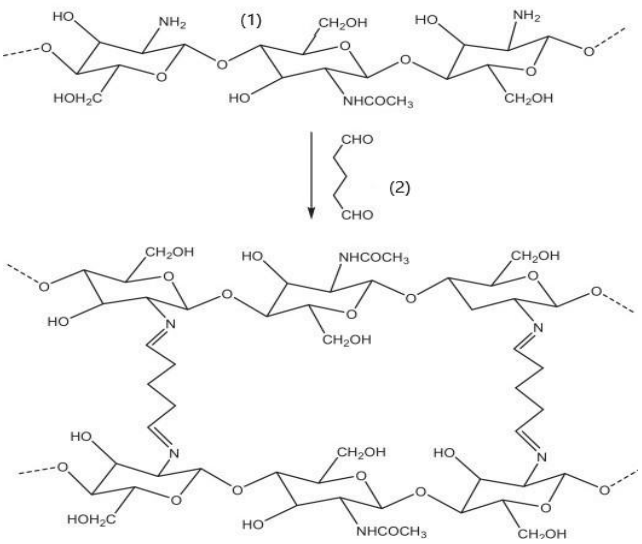

Figure 2.3.4: Crosslinking of chitosan (1) by glutaraldehyde (2) [35]

When glutaraldehyde is introduced to chitosan dissolved in acetic acid, and as the molar ratio of aldehyde/amine groups, R, are increased, the relatively weak self-associated network of chitosan is gradually replaced by a covalent network [61]. As shown by Monal et.al [61], the viscoelastic properties of chitosan hydrogel are dependent on the degree of crosslinking. They found that, despite being chemically crosslinked, the chitosan hydrogel displayed frequency dependent behaviour at low R's. For samples with a higher degree of crosslinking, the storage modulus of the gel was independent of frequency. The frequency dependent samples displayed the characteristics of a "weak" gel, as both the storage modulus and loss modulus increased with frequency. The authors attributed this behaviour to the dissolution of a chemically crosslinked network in a second entangled network that was formed by chitosan chains.

2.3.4 Gelatin hydrogel

Gelatin is the product of partial hydrolysis of the fibrous protein collagen [62]. Because of its properties, such as adhesiveness, plasticity, nonantigenity, and biocompatibility [2], gelatin is a good applicant in pharmacology, medicine and food industry. As described by Djabourov et.al [63], gelatin forms a physical thermoreversible gel at room temperature. By cooling the gel below 40°C, a sol-gel transition will occur, initiated by an increase in elasticity and viscosity. At this transition, a network of polymer chains that are responsible for the elastic properties of the gelatin gel advances. triple helical sequences will nucleate at random along the chains and form junctions between them. Once cooling is initiated, clusters of chains start

forming. However, the volume fractions of these chains are low, and the solutions exhibit Newtonian behaviour. After this point, shear stress applied to the solution will affect gelation kinetics. If the temperature is raised, the gel will return to a liquid state [63, 64].

Using gelatin as the sole gel-forming agent would be ill-advised due to its limitations concerning thermal stability, low mechanical strength, rheological properties and rate of structure formation [10, 63-65]. The viscoelastic properties of gelatin can be modified by using crosslinkers or combining it with other gelling compounds [2, 65]. Glutaraldehyde (GA) is widely used to crosslink proteins [66]. Studies performed by Oikawa and Nakanishi [36] seem to show that GA will affect the triple helices of gelatin. Although GA did not affect the size of the junction zones, which is vital for the gelation of gelatin, it reduced the number of nucleation sites of the triple helical structure, which caused a decrease in total crosslink density. Furthermore, Rathna et.al [10] proved an increased toxicity in GA crosslinked gelatin hydrogels.

There are two types of gelatin, type A and type B. Gelatin A is made by treating pigskin with acid over a short period of time. Gelatin B is made by treating bones or skin from cattle with calcium hydroxide over a longer period (1-3 months). The alkaline conditions cause hydrolysis of asparagine and glutamine to aspartic acid and glutamic acid, respectively, to occur more frequently during extraction of gelatine. This leads to gelatin B containing more acidic amino acids, giving it a lower IEP (isoelectric point) than gelatin A [67].

2.3.5 Chitosan-gelatin hydrogel

When crosslinked by glutaraldehyde, the hybrid polymer network is formed by imine groups, due to reaction of aldehyde groups with amino groups from both polymers [2]. Furthermore, the alkaline production conditions of gelatin B cause hydrolysis of aspargine and glutamine. When in an aqueous phase, residues of glutamic acid and aspartic acid interacts electrically with chitosan molecules, leading to hydrogen bonds being formed between the two polymers creating polyelectrolyte complexes [65]. The applicability of chitosan-gelatin (CG) hydrogels stem from the properties of the two polymers. Chitosan contributes with mechanical and antimicrobial properties, gelatin with cellular adhesion properties. Both polymers are biocompatible and biodegradable [10-12].

By varying the amounts of crosslinker and polymer, the properties of CG hydrogels can be easily manipulated. As shown by Peter et.al [68], increasing the concentration of chitosan in

CG scaffolds lead to a decrease in pore size, increase in scaffold density and an increase in swelling ability. Also, samples with higher concentrations of gelatin displayed lower densities and higher degradation rates.

Badawy et.al [69] examined characteristics of gel spheres containing chitosan, gelatin and algenate, crosslinked by glutaraldehyde. In a GA concentration range of 0,25-2%, it was found that 0,25% GA provided the highest degree of swelling (524%), whilst 2% GA provided the lowest degree (170%). The author suggests this is due to GA reacting with chitosan, rather than gelatin, forming crosslinking bridges, resulting in more crosslinks and a more compact wall and interior. More crosslinks would in turn hinder the mobility and relaxation of the polymer chains, reducing the free hydrodynamic volume in the polymer network that accommodates solvent molecules. This would prevent diffusion of solvent molecules and reduce the swelling degree [69-71]. The porosity of CG scaffolds has been shown to depend on GA concentration, as well as volume ratio of polymers [11].

2.4 Characterization of hydrogels

In the present study the different hydrogel systems were characterized by rheology, swelling studies and pulsed gradient spin-echo NMR. By means of these methods, mesh size, diffusion-coefficient, mechanical properties, and swelling degree was analysed.

2.4.1 Rheology

Rheology can be described as the science for describing the elastic, viscoelastic, and viscous properties of different materials [72]. Hydrogels are viscoelastic materials [32], which means that they display both elastic and viscous characteristics. The are many different rheometers and rheological measurements to choose from. In the present study the analysis of hydrogels will be performed by oscillatory testing on a rotational rheometer. The objective of rheological analysis is to understand how a material will deform related to microscopic structure and intermolecular interactions.

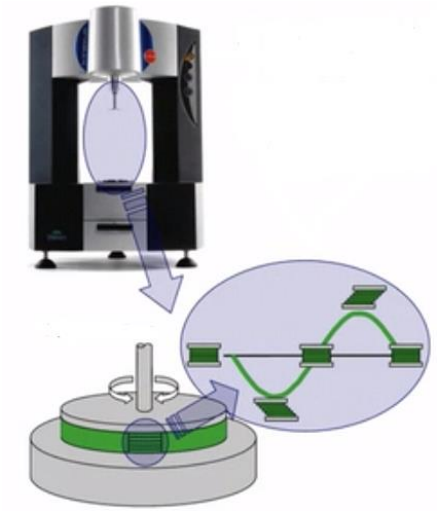

Figure 2.4.1: rotational rheometer with the sample highlighted in green. The measurement geometry is two parallel plates. The top plate oscillates back and forth, applying a sinusoidal signal to the sample. Illustration from Malvern Panalytical [73]

Some main quantities that are measured by oscillatory measurements need to be defined:

Shear stress is the amount of force applied to a given area of the sample

$$\tau = \frac{F}{A},$$

(1)

Where τ is shear stress (Pa), F is force (N) and A is area (m^2) [72].

When stress is applied, the resultant strain, which is the degree of deformation of the material, can be measured by the rheometer. Strain has no unit, but it is usually stated as a percentage.

$$\gamma = \frac{s}{h},$$

(2)

Where γ is strain, s is deflection path (m) and h is shear gap (m) [72].

The measure of stiffness of the material is called the complex modulus (G*) and is defined as the shear stress divided by the shear strain. The complex modulus consists of contributions from two component from the material response. The elastic component is the storage modulus (G') and the viscous component is the loss modulus (G''). The relationship between these two components define the behaviour of the material. If G' is larger than G'', the material displays solid behaviour. If the opposite is the case, the material behaves as a liquid. The storage modulus and the loss modulus are obtained directly when performing oscillatory measurements such as amplitude sweep and frequency sweep [73].

An amplitude sweep is a measurement that is performed at a fixed frequency and varying input amplitude, which is either stress or strain [73]. The purpose of an amplitude sweep is mainly to determine the limit of the linear viscoelastic region (LVE region) of the sample, and to analyse the structure of the material. The LVE region illustrates the range in which the measurement can be performed safely, without the sample being destroyed. Within the LVE region, G' and G'' values are used to determine the viscoelastic character. A larger G' illustrates a gel or solid-like structure, whilst a larger G'' indicates that the sample is in a fluid state [74]. The loss modulus (G'') values represent the part of the deformation energy that is lost due to internal friction. When the gel is moving beyond the limit of the LVE region, ruptures of bonds in the network of forces starts to occur. This leads to micro cracks in the gels structure, and broken fragments that can move freely. These fragments develop internal viscous friction that in turn convert deformation energy in to friction heat. With time, the individual micro cracks form a macro crack that continues throughout the gel. The viscous part of the viscoelastic behaviour will dominate (G'' > G'), and the gel will exceed the crossover point and start to flow [74]. The length of the LVE region are related to the toughness of the sample structure [73].

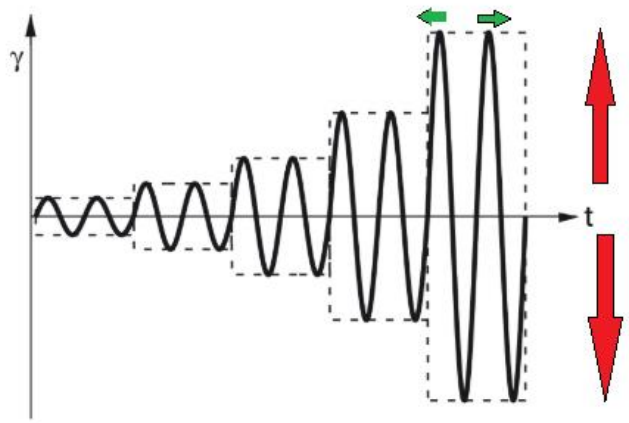

Figure 2.4.2: Illustration of an **a**mplitude-sweep measurement with controlled strain and a five step increase in amplitude. The frequency is kept constant at every measuring point. The amplitude is illustrated by red arrows, the frequency is illustrated by green arrows. Original illustration is from Anton Paar [74]

An amplitude sweep measurement is often displayed as a logarithmic plot of storage modulus (g') and loss modulus (G'') against strain as presented in figure 2.4.3.

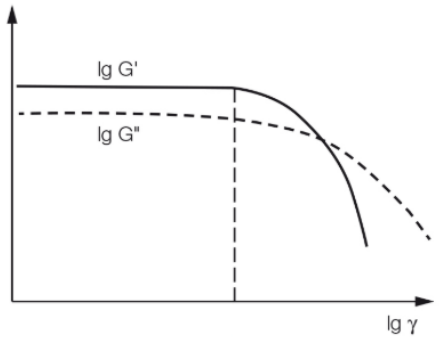

Figure 2.4.3: Storage modulus (G') and loss modulus (G'') against strain (γ). X-axis and Y-axis are on a logarithmical scale. The original illustration is from Anton Paar [74]

Once the LVE region of the sample has been determined, a frequency sweep measurement can be performed within the LVE region.

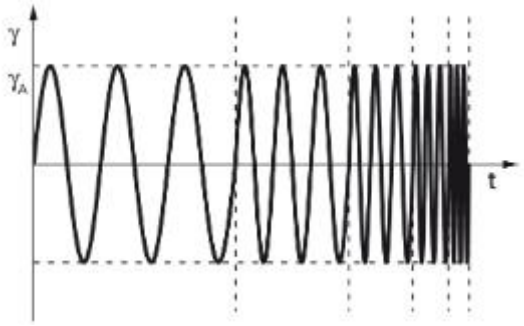

Figure 2.4.4: Example of a frequency sweep measurement. The strain is controlled while the frequency is increased in five steps. Illustration from Anton Paar [75]

The frequency sweep can be used to define the material by analysing their behaviour at rest i.e. as frequency goes toward zero. As illustrated in figure 2.4.5, a gel should display frequency-independent values of storage modulus and loss modulus. Furthermore, frequency sweep measurements are used to understand material behaviour at different timescales, where short timescales equals high frequencies and long timescales equals low frequencies [73].

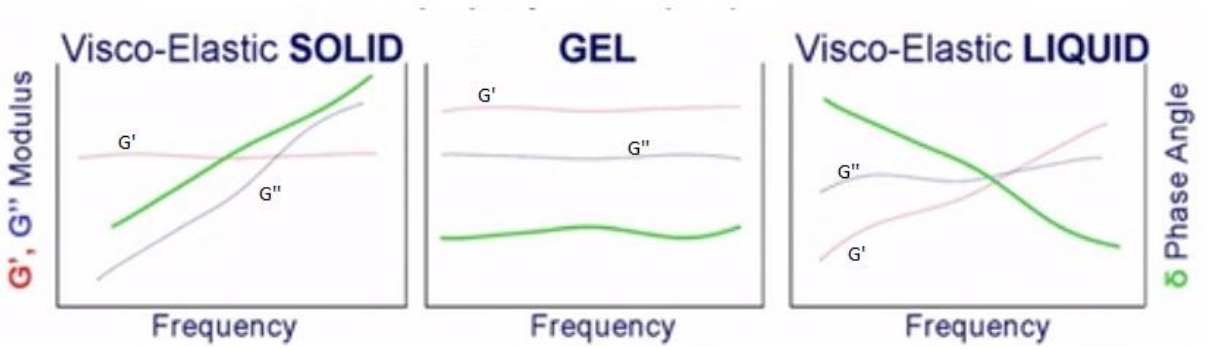

Figure 2.4.5: Example of different material behaviour analysed by frequency sweep measurements. As the frequency goes toward zero, the material can be described as at rest. Which of the two factors (G' and G'') that dominates at this stage, defines the behaviour of the material. For a viscoelastic solid, the storage modulus dominates at 0 Hz. For a gel, the behaviour is independent of frequency. For a viscoelastic liquid, the loss modulus dominates at 0 Hz. Original illustration is from Malvern Panalytical [73]

Another valuable test is a single frequency oscillation test, which is a measurement where both amplitude and frequency is kept at a constant. This way the changes in sample behaviour with external factors, such as time, can be monitored [73].

Mesh size based on rheological studies

The mesh size of poly(NIPAM-co-AAc) hydrogel can be estimated from rheological studies, based on Flory's theory of rubber elasticity of Gaussian chains [45, 76]. The equilibrium shear elastic modulus corresponds to the frequency independent elastic modulus (G') in the following way:

$$G' = A\left(\frac{\rho}{M_c}\right)RT \quad (3)$$

$$v_e = \frac{\rho}{M_c} \quad (4)$$

Where G' is the plateau value of the storage modulus, ρ is the polymer density, T is the temperature, R is the universal gas constant, A is the structure factor, M_c is the number average chain molecular weight, and v_e is the number of effective network chains per volume unit of polymer. A equals 1-2/f for a phantom network, where f is the functionality of the crosslinks [45, 77, 78]. v_e is related to the density of effective junctions n_e in the following way [45, 79]:

$$v_e = \frac{f}{2}\, n_e.$$

(5)

v_e, and subsequently the mesh size, can be calculated by adopting the approach of Wisniewska et.al [45], where one considers the volume element of the hydrogel to be a cube. The approach is based on the work of Haggerty et.al [80], which explains that the average spacing between neighbouring entanglements in the cubic volume element can be used for estimating mesh size, assuming that the junctions are evenly dispersed and are centrally positioned. Subsequently, the length (L) of a side of the cube and the mesh size at the initial state ($\xi_{c,i}^{rheo}$) can be expressed in the following way:

$$\xi_{c,i}^{rheo} = \frac{L}{2} = \left(\frac{RT}{G' N_A}\right)^{\frac{1}{3}},$$

(6)

where N_A is Avogadro's number.

As shown by Wisniewska et.al [45], by combining eq. (3), (4) and (5), the plateau value of the storage modulus (G') can be expressed as a function of the density of effective junctions (n_e) (eq. (7)). For calculating the density of effective junctions by using eq. (7), it is assumed that only one crosslink is formed per crosslinker molecule.

$$G' = n_e RT$$

(7)

2.4.2 PGSE NMR

The pulsed gradient spin echo (PGSE) NMR experiment is a diffusion NMR technique developed by E.O. Stejskal and J.E. Tanner in 1965 [81]. Diffusion NMR combines radiofrequency pulses (rf-pulses) with magnetic field gradients that encode spatial information. The experiment is helpful for measuring diffusion coefficients, which are subsequently used to calculate mesh size of the analysed material. Although a very useful characterization method, PGSE NMR does have some limitations. Due to the entire volume of the sample being analysed, the experiment is sensitive to heterogeneity in the sample [82]. Furthermore, probe diffusion experiments are sensitive to the size of the diffusing probe molecules [83].

Self-diffusion is described by Peter Stilbs [84] as the net result of the thermal motion-induced random walk process experienced by particles or molecules in solution. The self-diffusion coefficient (D), characterizes the gaussian radial distribution function of molecules respecting their original positions in an infinitely large system altogether. Normally, self-diffusion coefficients in liquid systems range from $10^{-9}\ m^2\ s^{-1}$ to $10^{-12}\ m^2\ s^{-1}$. Typically, they do not significantly depend on temperature or concentration [84].

There are different types of PGSE NMR experiments, but some features are constant. An illustration of a basic PGSE NMR experiment is given in figure 2.4.6.

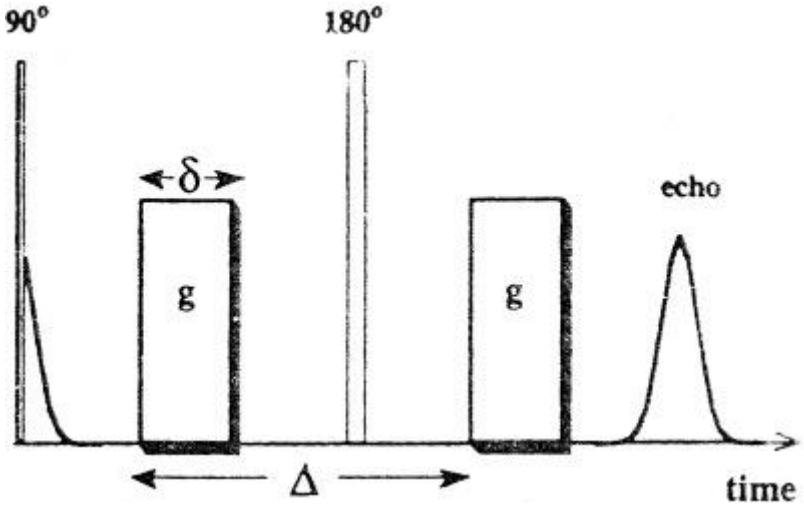

Figure 2.4.6: Pulse sequence in the PGSE NMR experiment. The magnetization is excited by the 90 ° rf-pulse. Subsequently, the gradient pulse is applied to disperse the magnetization and to give each spin a position dependent phase. During a period of $\frac{\Delta}{2}$, diffusion takes place, before the 180° rf-pulse inverts the dispersed magnetization. The second gradient pulse is applied to refocus the signal [82]. Illustration from Li et.al [85]

Diffusion coefficients can be computed by using the Stejskal-Tanner equation [81]:

$$\frac{I}{I_0} = e^{-\gamma^2 g^2 \delta^2 \left(\Delta - \frac{\delta}{3}\right) D}$$

(8)

Where I/I_0 is the signal attenuation, γ is the gyromagnetic ratio (26,7522 x 10^7 rad T^{-1} s^{-1} for ^1H), g is gradient strength, Δ is the effective diffusion time, δ is the effective gradient pulse width, and D is the diffusion coefficient (m^2/s). The magnitude of the diffusion coefficient is given by

$$D = \frac{k_B T}{f},$$

(9)

where k_B is Boltzmann's constant, T is absolute temperature and f represents the frictional factor. f is given by the Stokes equation:

$$f = 6\pi\eta r,$$

(10)

That can be combined with eq. (9) to give the Stokes-Einstein relation:

$$D = \frac{k_B T}{6\pi\eta r}.$$

(11)

For references to eqs. (9-11) see Atkins and De Paula [86].

Diffusion of probe molecules in hydrogels is slower than its diffusion in solution. This is because diffusion is mainly taking place within water-filled regions in space defined by the polymer chain, where higher fractal resistance and asymmetry is slowing down the diffusion [45]. This diffusion can be expressed as the diffusion quotient ($\frac{D_g}{D_0}$), where D_g is the restricted diffusion of probe molecules due to being trapped in the polymer network, and D_0 is the unrestricted diffusion of the same molecule in solution. The mesh size (ξ) of the hydrogel can be obtained by relating the diffusion coefficient to the mesh size in the following way [45]:

$$\frac{D}{D_0} = \exp(-\frac{r_s}{\xi}).$$

(12)

This way, the mesh size of the hydrogel can be obtained indirectly by comparing the diffusion coefficient of the probe molecule in the hydrogel, to the diffusion coefficient of the probe molecule in a dilute solution [45].

The hydrodynamic radius of the probe molecule (r_s) can be obtained through the following equation:

$$r_s = \frac{k_B T}{6\pi\eta D_0} \quad (13)$$

with η being the viscosity of D_2O (1,093 mPa s) at 298 K [87]

Furthermore, combining the expression for r_s with eq. (12), one gets an expression where the mesh size of hydrogels can be obtained through PGSE NMR analysis:

$$\xi^{NMR} = \frac{K_B T}{6\pi\eta D_0} \left(\ln \frac{D_0}{D_g}\right)^{-1} \quad (14)$$

2.4.3 Swelling

The ability to absorb and retain water or biological fluid is a property that define hydrogels. The degree of swelling displayed by hydrogels is an uncomplicated and useful characterization method, as it presents information about the structure of the system such as degree of crosslinking and the subsequent mesh size, as well as physical properties such as temperature-and pH-responsive behaviour. Furthermore, it is a simple method of studying the influence of synthesis parameters and chemical composition on the hydrogel [28, 34, 40]

In the present study, mass swelling ratio (Q_m) and water content (W_c) of the hydrogels were determined by eqs. (15 and 16), respectively.

$$Q_m = \frac{W_s}{W_d} \quad (15)$$

$$W_c = \frac{W_s}{W_d} * 100\% \quad (16)$$

Mesh size based on swelling studies

Flory's theory is used to determine the mesh size of a hydrogel through swelling studies. The mesh size of a hydrogel in the swollen state (ξ^{SW}) is related to the root mean-square end-to-end distance of the polymer subchain between to crosslinking points in the undisturbed state ($\sqrt{(r_0^2}$), as shown in eq. (17).

$$\xi^{SW} = (v_{2s})^{-\left(\frac{1}{3}\right)}\sqrt{(r_0^2}),$$

(17)

Where v_{2s} is the volume fraction of the polymer, which is equal to the mutual value of the volumetric swelling degree (Q_v^{-1}). $\sqrt{(r_0^2}$) is calculated by using the following expression:

$$\sqrt{(r_0^2}) = l\left(\frac{2M_c}{M_0}\right)^{\frac{1}{2}} C_N^{\frac{1}{2}},$$

(18)

where l is the length of a C-C bond ($l = 0{,}154\ nm$), M_C is the molar mass of the subchain between two crosslinking points, M_0 is the molar mass of the monomer and C_N is Flory's characteristic ratio.

The molar mass of the subchain between two crosslinking points (M_C) is given by the average molar mass of monomers (M_0) and the degree of crosslinking (d_c) as

$$M_C = \frac{1}{2} M_0 d_c^{-1}\ ,$$

(19)

and

$$d_c = \frac{n_{DAT}}{n_{NIPAM}+n_{AAc}+n_{DAT}}$$

(20)

Where n_{DAT}, n_{NIPAM} and n_{AAc} are the number of moles of DAT, NIPAM and AAc, respectively.

By rearranging eq. (19) we get the following equation:

$$d_c^{-\frac{1}{2}} = \left(\frac{2M_c}{M_0}\right)^{\frac{1}{2}},$$

(21)

Furthermore, eq. (18) can now be expressed as:

$$\sqrt{(r_0)^2} = l(d_c)^{-\frac{1}{2}}(C_N)^{\frac{1}{2}}$$

(22)

The volumetric swelling ratio (Qv) can be obtained by measuring the increase of the weight of the hydrogel during the swelling process in the following manner:

$$Q_v^{-1} = \frac{\frac{1}{\rho_{pol}}}{\frac{Q_m}{\rho_{solv}} + \frac{1}{\rho_{pol}}},$$

(23)

Where Qm is the mass swelling ratio and ρ_{pol} and ρs_{olv} are the densities of the hydrogel and the solvent, respectively.

For gel swollen in water at 298 K:

$\rho_{pol} = 1{,}1\ g\ mL^{-1}$

$\rho_{solv} = 1{,}0\ g\ mL^{-1}$

Finally, the mesh size of the hydrogel can be calculated using the following equation:

$$\xi^{SW} = l\left(\frac{n_{DAT}}{n_{NIPAM}+n_{AAc}+n_{DAT}}\right)^{-\frac{1}{2}} C_N^{\frac{1}{2}}\left(\frac{Q_m\,\rho_{pol}}{\rho_{solv}} + 1\right)^{\frac{1}{3}}$$

(24)

For references for eqs (17-24), see Wisniewska et.al [45] and references cited therein.

3 Experimental

3.1 Materials and methods

Table 3.1.1: Overview of the materials used for analysis and synthesis of the different hydrogel systems

Systems	Name	Product number (Sigma Aldrich)	M_w
Poly(NIPAM-co-AAc) hydrogel			
	Acrylic acid	147230	72.06 g mol^{-1}
	N-isopropylacrylamide (NIPAM)	731129	113.16 g mol^{-1}
	Ammonium persulfate (APS)	A7460	228.20 g mol^{-1}
	N,N,N',N'-tetramethylethylenediamine (TEMED)	411019	116.20 g mol^{-1}
	(+)-N,N'-Diallyltartramide (DAT)	156868	228.25 g mol^{-1}
SA-CS hydrogel			
	Thioglycolic acid	528056	92.12 g mol^{-1}
	4-maleimidobutyric acid	63174	183.16 g mol^{-1}
	N-(3-dimethylaminopropyl)-N'-ethylcarbodiimide hydrochloride (EDAC)	E1769	191.70 g mol^{-1}
	N-hydroxysuccinimide (NHS)	130672	115.09 g mol^{-1}
	Chitosan	C3646	-
Chitosan-gelatin hydrogel			
	Gelatin B	G9391	40-50 kDa
	Chitosan	419419	310-375 kDa

	Glutaraldehyde solution (25% in H_2O)	G6257	100.12 g mol^{-1}
	Sodium sulfate	239313	142.04 g mol^{-1}
	Acetic acid	-	60,05
NMR analysis			
	D2O	151882	20,03
	B-cyclodextrin	C4767	1134,98

3.2 Preparation of hydrogels

In this section the preparation and chemical composition of the different hydrogel systems will be presented

3.2.1 Poly(NIPAM-co-AAc) hydrogel

The following procedure was based on the work of Wisniewska et.al [45].

Poly(NIPAM-co-AAc) hydrogels were synthesized by free radical polymerization in aqueous solution. The monomers, NIPAM and acrylic acid, were crosslinked by DAT, whilst the redox couple APS/TEMED functioned as initiator. The monomers, DAT, and APS were dissolved in 5 mL milli Q water before being cleaned in an ultrasonic bath for 10 minutes. The solution was then subjected to 5 minutes of nitrogen bubbling for deoxygenation. 6,63 M TEMED was added and the reaction was carried out at room temperature overnight.

Table 3.2.1: chemical composition of Poly(NIPAAm-co-AAc) hydrogels. M is molar concentration, TEMED:APS ratio is referred to molar concentration

APS (M)	*NIPAM (M)*	*AAc (M)*	*DAT (M)*	*TEMED:APS*
0,018	0,669	0,033	0,018	8 : 9

After synthesis the hydrogels were incubated in milli Q water for one week with daily substitution of water to remove unreacted monomers. The hydrogels were subsequently dried at room temperature until a stabile weight was reached.

The formulation of poly(NIPAM-co-AAc) hydrogel presented in table 3.2.1 was used for NMR and rheological analysis. The ratio between the initiators was varied for swelling studies.

3.2.2 Self-assembling chitosan hydrogel

The following procedure was based on the work of Kiene et.al [49].

Thiolation of chitosan

Chitosan was dissolved in 10mL H_2O (0.5% w/v) and the pH was adjusted to 5,5 with 1 M HCl. 1,1% (v/v) of thioglycolic acid was added to the solution, along with EDAC and NHS in the same molarity. The solution was stirred over night at room temperature.

Maleimide coupling

4-maleimidobutyric acid was dissolved in DMS (80% w/v) resulting in a concentration of 0,8% (w/v) and added to 10mL chitosan solution (pH adjusted to 5,5 with 1 M HCl). EDAC and NHS were added in the same molarity as 4-maleimidobutyric acid. The reaction was stirred overnight at room temperature.

Both modified polymers were purified by dialysis at 4 °C, the dialysis setup is presented in table 3.2.2. The membranes molecular weight cut off was 14 kDa. Both Mal-CS and SH-CS were recovered by freeze-drying (lyophilization).

Table 3.2.2: Dialysis setup for the two modiefied polymers SH-CS and Mal-CS

Dialysis solution	Time (days)
5mM HCl	3
5mM HCl + 1% NaCl	2
1mM HCl	2

30 mg/mL of lyophilised SH-CS and 13,5 mg/mL of lyophilised Mal-CS respectively, were dissolved in H_2O and the solutions were formed by stirring overnight at room temperature. Subsequently, the solutions were mixed in a 1:1 ratio, referred to the weight of lyophilised CS, and set to crosslink overnight at room temperature.

3.2.3 Chitosan hydrogel

1% w/v chitosan was added to 2% v/v acetic acid by magnetic stirring at room temperature for 24 hours. The polymer solution was filtered through a 0.45 µm filter using a syringe, to ensure removal of unsolved particles. Six samples of 5 mL polymer solution were prepared

Table 3.2.3: Chemical composition of chitosan hydrogels samples 1-4. Each sample contained 5 mL polymer solution

Sample	Glutaraldehyde (% v/v)	Na_2SO_4 solution ($\boldsymbol{mol * L^{-1}}$)
C1	0,74	0,05
C2	0,74	0,04
C3	0,8	0,05
C4	0,8	0,04

To avoid a confined and local cross-binding by glutaraldehyde (GA), and thus inhomogeneous gel-formation, the samples were manually shaken immediately after the addition of GA. Furthermore, the samples were centrifuged (5 min at 2000 rpm) twice, with the samples being shaken in between. To allow for complete cross-binding, the samples were put to rest for minimum one hour before Na_2SO_4 solution was added. 10 mL Na_2SO_4 solution was added to each sample. Three parallels of each sample were prepared for swelling studies.

Another experiment was performed, where $\frac{1}{10}$ amount of GA was used while all other parameters were kept constant. While this was initially done by mistake, it did provide an opportunity to investigate how the crosslinking is affected by such a strongly reduced amount of GA.

3.2.4 Gelatin hydrogel

1% w/v gelatin was dissolved in 2% v/v acetic acid solution by magnetic stirring for 24 hours. The polymer solution was subsequently filtered through a 0,45 µm filter using a 5 mL syringe. The solution was rested at 40 °C overnight. Glutaraldehyde was added to each of the samples as described in table 3.2.4.

Table 3.2.4: Chemical composition of gelatin hydrogel samples 1-4. Each sample contained 5 mL polymer solution

Sample	**Glutaraldehyde (% v/v)**	**Na_2SO_4 ($mol * L^{-1}$)**
G1	0,74	0,05
G2	0,74	0,04
G3	0,8	0,05
G4	0,8	0,04

The samples were manually shaken directly after addition of glutaraldehyde. They were then centrifuged as described in section 3.2.3. The samples were rested for approximately one hour before 10 mL of Na_2SO_4 solution was added.

3.2.5 Chitosan-gelatin hydrogel

The following procedure was based on the work of Liu et.al [11].

Granules of chitosan and gelatin were dissolved separately in 2 % v/v acetic acid. The polymer solutions were subsequently mixed and allowed to rest for 24 hours. The polymer solution was filtered through a 0,45 µm filter using a 5 mL syringe to ensure a fully dissolved polymer solution, before glutaraldehyde was added to the samples as presented in table 3.2.5.

Table 3.2.5: Chemical composition of chitosan-gelatin hydrogels samples 1-4. Each sample contained 5 mL polymer solution

Sample	Glutaraldehyde (% v/v)	Na_2SO_4 solution ($mol * L^{-1}$)
1	0,74	0,05
2	0,74	0,04
3	0,8	0,05
4	0,8	0,04

At this point, different hydrogel formulations and steps of synthesis was attempted. Table 3.2.6 provides an overview of the three different systems.

Table 3.2.6: Overview of the three systems of chitosan-gelatin hydrogel that was studied. P is the total amount of polymer in acetic acid solution, C:G is the ratio of chitosan and gelatin referred to mass, and T is the temperature at which the solutions were rested before addition of Na_2SO_4 solution

Formulation	P (% w/v)	C:G (g)	T (°C)
X	2,5	4,5 : 1	50
Y	1	1 : 1	50
Z	1	1: 1	22

The polymer solutions were rested for approximately one hour before addition of Na2SO4 solution. Samples were allowed to crosslink overnight.

3.3 Methods

The experimental methods and equipment used to synthesize the hydrogel systems are presented.

3.3.1 Rheology

Oscillatory measurements were performed on a Kinexus rheometer (Malvern Panalytical, Great Britain), using the cone-plate and parallel-plate measuring systems. The rotational bobs utilised were CP4/40 SR1454 SS and PU20 SR1426 SS for cone-plate and parallel-plate, respectively.

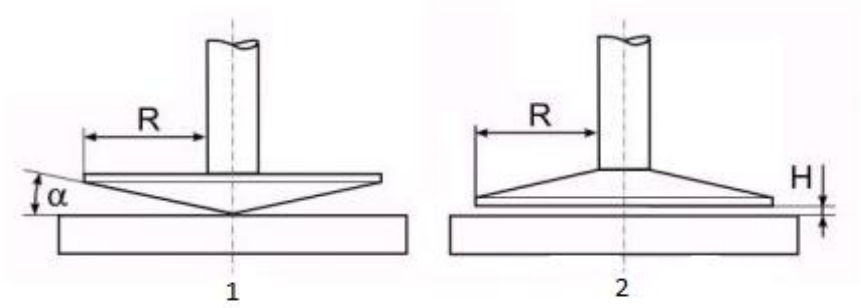

Figure 3.3.1: Cone-plate (1) and parallel-plate (2) measuring systems. Illustration from Anton Paar [88]

Amplitude sweep measurements were performed to determine linear viscoelastic region (LVE region), and for evaluating the samples viscoelastic character. Shear strain range was 0,1-100% at a preset frequency of 1,0 Hz. Frequency sweep measurements were performed to analyse the behaviour of the samples at rest, and at different timescales within the LVE region. Shear strain was controlled at 1% while frequency varied within a range of 0,1-10 Hz. Gap between the rotational bob and plate was set at 2 mm for parallel-plate measurements. Measurement temperature was 25 °C for all samples and measurements.

3.3.2 Swelling studies

To determine swelling ratio and water content percentage, hydrogel samples were incubated in beakers with excess amount of distilled water at room temperature. Periodical measurements were performed where hydrogels were superficially dried using filter paper, and water was replenished. The sequence was carried out until hydrogels were completely saturated, i.e. until the weight was stable. Dry weight (W_d) and saturated weight (W_s) was recorded. Mass swelling ratio (Q_m) and water content (W_c) was determined by eqs. (15 and 16), respectively.

3.3.3 PGSE NMR studies

PGSE NMR was carried out on a Bruker Ascend 500 WB spectrometer (Rheinstetten, Germany) operating at a proton frequency of 500 MHz. The spectrometer was equipped with a diff30 NMR probe, and measurements were performed at 298 k using a stimulated echo sequence with bipolar field gradient pulses (DiffSteBp).

The hydrogels were dried in air until no more weight loss was registered. They were subsequently incubated in 9,5 mM β-Cyclodextrin solution prepared in D_2O until swelling

equilibrium was reached, and then placed in standard 5 mm NMR tubes. β-Cyclodextrin was used as the probe molecule for probe diffusion experiments.

Regarding the diffusion experiments, the signal intensity was recorded as a function of gradient strength (g) at 16 different values. The maximum value of g (g_{max}) was set at 205 G/cm. The diffusion time (Δ) and gradient duration time (δ) were fixed at 10 and 2 ms, respectively.

3.3.4 Freeze-drying

Freeze-drying (lyophilization) is a gentle drying method that is used to mitigate denaturing processes that occur in some compounds, as well as creating porous scaffolds with interconnecting pores [89]. Pre-freezing is a method where the sample is stored at a low temperature for a given amount of time before it is lyophilized. It has been shown to have an effect on mean pore sizes of biopolymer hydrogels [89]

In the present work, the samples were lyophilized using a Christ Alpha 1-2LD plus (Osterode, Germany) at -50 °C for 48 hours.

4 Results and discussion

The results gained from this study will be presented and discussed in this chapter. The chapter is organized by sections, where the different hydrogel systems are presented, and subsections where results gained from rheological studies, swelling studies, and NMR studies are discussed for each hydrogel system.

4.1 Poly(N-isopropylacrylamide-co-acrylic acid) hydrogel

4.1.1 Rheology

For the purpose of rheological characterization, all poly(NIPAM-co-AAc) hydrogel samples were synthesized in situ, and then allowed to rest before rheological analysis. The LVE region of the hydrogels of this particular composition was already known, due to the work of Wisniewska et.al [45]. Therefore, the rheological analysis that was performed during this study consists of frequency-sweep tests performed at 1% strain at varying time intervals.

Table 4.1.1: Overview of the hydrogel systems that are analysed by rheology in this section. t is the amount of time between synthesis and frequency sweep measurement. Hydrogels A and B have the same chemical composition, which is described in section 2.1.5

Hydrogel	t (hours)
A	24
B	1

Firstly, a frequency-sweep was performed on hydrogel A (figure 4.1.1).

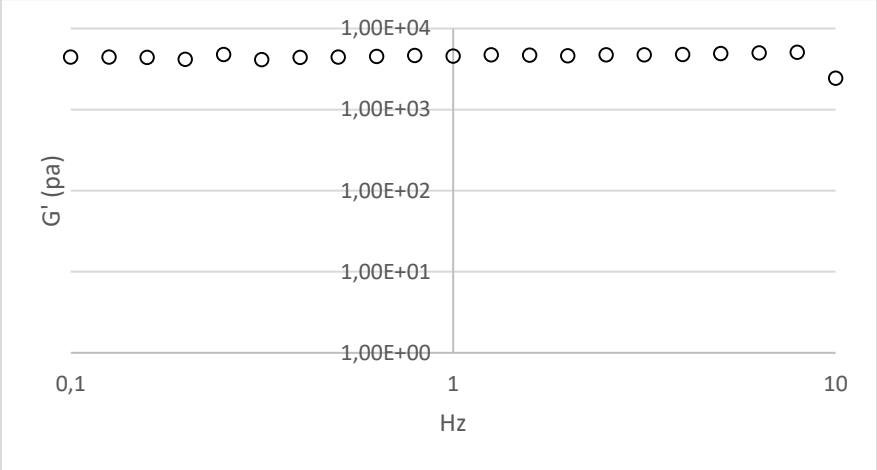

Figure 4.1.1: Characterization of the storage modulus as a function of frequency for poly(NIPAM-co-AAc) hydrogel A. Strain was fixed at 1%. The hydrogel was synthesized in situ and allowed to rest for 24 hours to ensure complete network formation before analysis.

The storage modulus values (G') exhibit a nearly frequency independent behaviour within the applied frequency range, indicating an elastic and mechanically strong hydrogel. Hydrogels that show this behaviour can be classified as "ideal hydrogels", and it makes it possible to estimate their microstructure based on the theory of rubber elasticity [eqs. (5) and (6)] [40, 76]. Furthermore, the storage moduli value at 1 Hz is around $4{,}6 * 10^3\ Pa$, which is relatively large compared to values found in literature for the same hydrogel formulation ($8{,}8 * 10^2\ Pa$) [45]. The two hydrogels have the same ratio of total polymer concentration (T%) to crosslinker concentration (C%), they were synthesized at room temperature, and frequency sweep were performed on the same rheometer with identical parameters. Therefore, it is likely that the difference in storage modulus stem from polymerization time. Frequency sweep measurements by wisniewska et.al [45] were performed directly after synthesis, and continued for a maximum of 4 hours. Polymerization of the hydrogel network is possibly still ongoing at this time, which could explain the much larger G' values found after 24 hours in the present study.

To investigate this hypothesis, a frequency sweep sequence was designed to run constantly for 24 h. This sequence also allowed us to study the potential effect of continuous strain on the gelation process. Two parallels of poly(NIPAM-co-AAc) hydrogel are compared in figure

4.1.2. The figure illustrates the disparity in storage modulus (G') based on polymerization time.

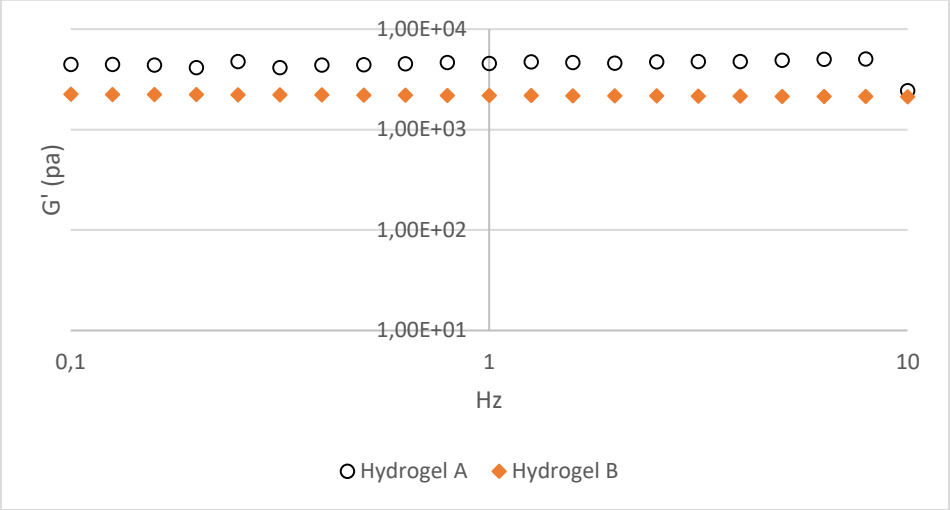

Figure 4.1.2: Characterization of the storage modulus as a function of frequency for hydrogels A and B. The two parallels differ in polymerization time as the measurements were made 24 hours after synthesis in the case of hydrogel A, and one hour after synthesis in the case of hydrogel B. Strain was fixed at 1%.

Comparing the storage moduli values at 1 Hz for the two parallels, there is a 109% increase between the first hour after synthesis and 24 hours after synthesis, indicating that a longer polymerization time leads to better mechanical strength. This is in line with the findings of Denisin and Pruitt [7]. However, the G' values displayed by hydrogel B are significantly larger than values reported by Wisniewska et.al [45] for the same hydrogel formulation with comparative polymerization time. The reasons for the disparity are unclear.

To monitor the polymerization process and get a clearer picture of the evolution of the hydrogel network, the storage modulus and loss modulus of hydrogel B was characterized as a function of time (figure 4.1.3).

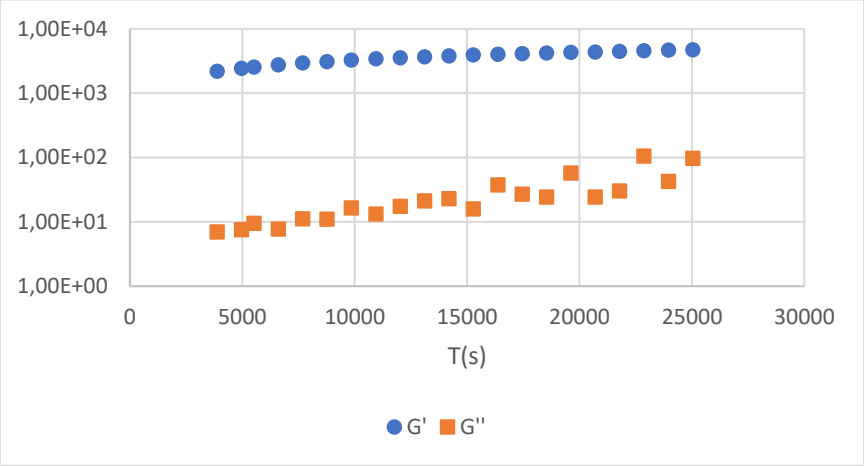

Figure 4.1.3: Characterization of the storage modulus (G') and the loss modulus (G'') as a function of time for hydrogel B. Strain and frequency is 1% and 1 Hz, respectively, for all datapoints. The period of analysis was 1-7 hours after synthesis

The hydrogel was rested for one hour before analysis was initiated, the exact point of gelation ($\tan \delta = G''/G' = 1$) is not observable, indicating that the gelation point had already been reached. Therefore, gelation must have occurred within 60 minutes after in situ synthesis. The absence of the rapid increase in modulus that is expected after gelation, is in line with the assumption that 90 % of acrylamide molecules are polymerized within 1 hour in chemically initiated radical polymerization [7].

TEMED to APS ratio for this hydrogel formulation was 8 : 9 referred to molar concentration of the initiators. As described previously, the molar ratio of TEMED and APS affect the gelation time of the hydrogel (see section 1.5). For a poly(isopropylacrylamide) hydrogel crosslinked by N,N'-methylenebisacrylamide and prepared by free radical polymerization using APS and TEMED in a 1 : 1 ratio, Adrus et.al [40] found that gelation occurred around 250 minutes after in situ polymerization. Furthermore, reducing TEMED to APS ratio lead to longer lag periods before gelation. The quick onset of gelation for our formulation could be caused by acrylic acid. Co-polymer hydrogels of NIPAM and acrylic acid have already been proven to exhibit significantly different properties than their homopolymer counterparts, such as pH and temperature sensitivity [6].

G’ values displayed a slow and steady increase up toward an equilibrium value as the polymerization time increased. After seven hours of continuous frequency sweep measurements, the measurements turned unstable. The data that was gained after this point will not be included in this study, as the validity of it is questionable. The loss of water that was observed during the rheological analysis, might have produced a dry and inhomogenous sample that could cause faulty measurements.

The frequency independent behaviour of hydrogels A and B, and Flory’s theory of rubber elasticity of gaussian chains allows for the analysis of the microstructure of the hydrogels[45, 76]. The mesh sizes at the initial state were estimated by using eqs. (5-7). The theoretical functionality (f) of the crosslinker (DAT) is 4, as each DAT molecule have four functional groups capable of reacting with four polymer segments.

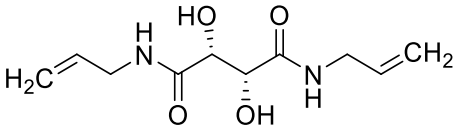

Figure 4.1.4: (+) N,N’-Diallyltartramide (DAT)

The intention was to compare the microstructure of the two parallels after equal polymerization time, i.e. 24 hours after synthesis. Due to the unstable measurements, any data recorded for hydrogel B after 7 hours was deemed not reliable. Therefore, the plateau value of the storage modulus (G’) that was recorded 7 hours after synthesis (figure 4.1.5), was used to calculate the mesh size of hydrogel B (table 4.1.2)

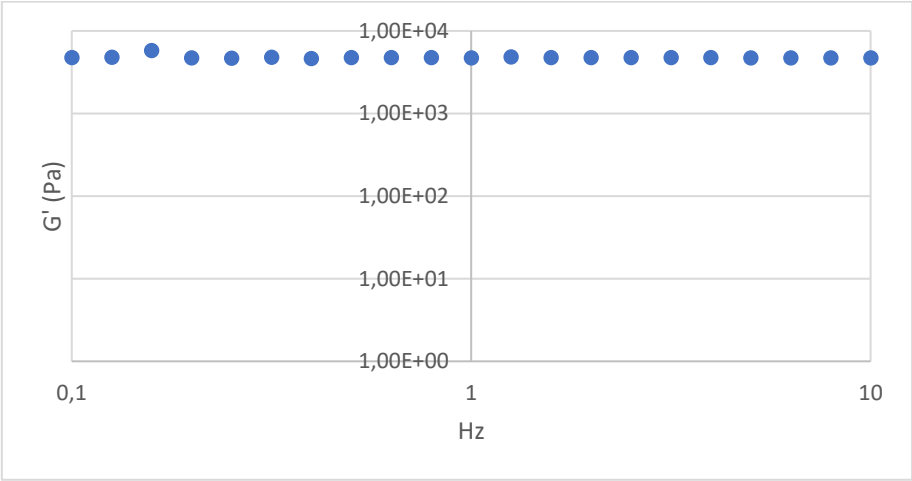

Figure 4.1.5: Characterization of the storage modulus as a function of frequency for hydrogel B. Strain was fixed at 1%. The measurement was recorded 7 hours after synthesis

Table 4.1.2: Storage modulus (G'), density of effective junctions (n_e), and calculated mesh size assuming a cubic-shaped volume element (ξ_c^{rheo}).

Sample	$\boldsymbol{G'(Pa)}$	$\boldsymbol{n_e(mol\, m^{-3})}$	$\boldsymbol{\xi_c^{rheo}(nm)}$
Hydrogel A	$4{,}56 * 10^3$	1,84	9,7
Hydrogel B	$4{,}73 * 10^3$	1,91	9,5

The connection between storage modulus and mesh size is reflected in the equation model. Comparing the storage moduli values and mesh sizes for hydrogels A and B, there is no indication that the application of continuous strain would have any effect on the mechanical properties of the hydrogel. This is expected, as the applied strain was within the LVE region of the hydrogel. The storage moduli values of hydrogels A and B are quite similar, suggesting that polymerization of the hydrogel network had essentially been completed after seven hours.

4.1.2 Swelling studies

Swelling studies were performed with varying TEMED to APS ratios to investigate the potential effect on swelling behaviour. Two poly(NIPAM-co-AAc) hydrogels with differing concentration of initiators were synthesized. Mass swelling ratio and water content of the hydrogels are shown in table 4.1.3. A visual presentation of mass swelling ratios is displayed in figure 4.1.6.

Table 4.1.3: swelling studies of two poly(NIPAM-co-AAc) hydrogels. Three parallels of each formulation were analysed

TEMED:APS ratio	W_d ***(g)***	W_s ***(g)***	Q_m	W_c ***(%)***	***A (mM)***
8 : 9	0,0814	8,9319	109,7	10973	18
8 : 9	0,1192	12,015	100,8	10080	18
8 : 9	0,1821	19,439	106,7	10675	18
9 : 1	0,0368	7,0351	191,2	19117	1,75
9 : 1	0,183	35,944	196,4	19641	1,75
9 : 1	0,1515	29,034	191,6	19164	1,75

Dry weight (W_d), saturated weight (W_s), mass swelling ratio (Q_m), APS concentration (A), and water content (W_c) of poly(NIPAM-co-AAc) hydrogels synthesized with TEMED to APS ratios of 8 :9 and 9 : 1, respectively. Initiator ratios are referred to molecular concentration

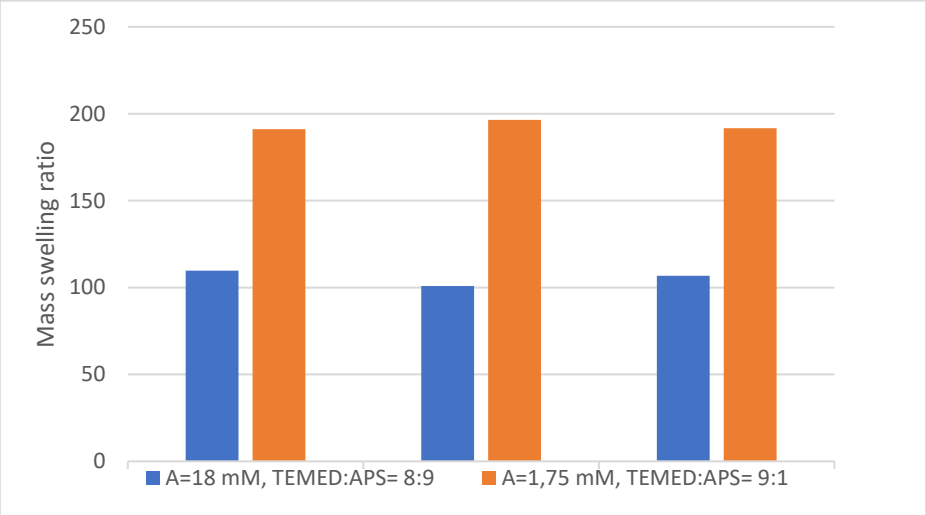

Figure 4.1.6: Mass swelling ratio of two poly(NIPAM-co-AAc) formulations. A is the molecular concentration of APS

The water content and swelling degree of the hydrogels increased by 83% on average as APS concentration (C) decreased from 18 mM to 1,75 mM. The decrease in amount of APS lead to a consistent increase in swelling. Referring to the work of Adrus et.al [40] who found minimal correlation between the ratios of initiators and swelling, and produced hydrogels exhibiting total swelling degrees (Q_m) of around 10, it would seem that the introduction of acrylic acid as comonomer has a significant effect on both total swelling degree and swelling mechanics. The weight percentage of AAc influences the pore size of poly(NIPAM-co-AAc) hydrogel [44]. In the present study, poly(NIPAM-co-AAc) was originally considered a neutral hydrogel, as the molar ratio of NIPAAm to AAc is 95-5. Consequently, the swelling behaviour of the hydrogel was thought to only derive from the water-polymer thermodynamic mixing contribution to the overall free energy which is coupled with an elastic polymer contribution [13]. Nevertheless, the carboxylic acid groups on the poly acrylic acid chain associate strongly with water molecules, possibly enhancing the swelling ability of the poly(NIPAM-co-AAc) hydrogels.

To investigate the role of acrylic acid, we compared the swelling data from this study with swelling data found by Gao et.al [90] for poly(NIPAM-co-AAc) hydrogel. Hydrogel formulation in both studies are similar, although not identical. Theoretical polymer concentration per hydrogel is approximately 89%, referred to mol%, in both studies. Ratio of initiator concentration differs more significantly, as TEMED to APS ratio is 1 : 4.4 in Gao's study, compared to either 8 : 9 or 9 : 1 in the present study. The hydrogels displayed swelling degrees of less than 20 at 25 °C and pH 6,8 [90].

Now, the significant difference in swelling is interesting. The swelling behaviour found in the present study is in line with results found by Wisniewska et.al [45] for the same hydrogel formulation. The relatively limited swelling found by Gao et.al could stem from the large amount of APS compared to TEMED. Furthermore, from the work of Elliott et.al [34], we know that the water concentration during polymerization of the hydrogel network affects the crosslinking of the network due to cyclization reactions. Less water leads to more crosslinked networks, which in turn leads to less swelling. The disparity in water concentrations between the present study and Gao et.al, 138 mg/mL compared to 95 mg/mL, respectively, alongside initiator concentrations, are likely reasons for the disparity in swelling behaviour.

Mesh sizes based on dynamic swelling were calculated. The equilibrated volumes of hydrogels with different initiator concentrations were used for obtaining the mesh size using eq. (24). Results are presented in table 4.1.4.

Table 4.1.4: Mesh sizes at equilibrium. Amount of initiator (APS) was varied between samples.

A (mM)	Q_{ms}	$\sqrt{r_0^2}\ (nm)$	$\xi_{eq}^{SW}\ (nm)$	**TEMED:APS**
18	109,7	2,1	10,2	8 : 9
18	100,8	2,1	9,9	8 : 9
18	106,7	2,1	10,1	8 : 9
1,75	191,2	2,1	12,3	9 : 1
1,75	196,4	2,1	12,4	9 : 1
1,75	191,6	2,1	12,3	9 : 1

A is the initiator (APS) concentration in the hydrogels, Q_{ms} is the swelling ratio at equilibrium, ξ_{eq}^{SW} is the mesh size at equilibrium, TEMED:APS is the ratio between initiators, referred to molecular concentration, and $\sqrt{r_0^2}$ is the root mean-square end-to-end distance of the polymer subchain between to crosslinking points in the undisturbed state.

The variation of swelling with initiator concentration was clearly linked, meaning that a larger disparity in the ratio of TEMED to APS lead to more swelling. Subsequently, the mesh size follows the same trend, as hydrogels with higher swelling degrees also displays a larger mesh size. Due to comparable hydrogel formulation, the three parallels with TEMED to APS ratio 8 : 9 can be compared with results found in literature. The mesh size found by Wisniewska et.al [45] was 13 nm. The disparity in mesh size is related to the smaller mass swelling ratio for the hydrogels in the present study. This is expected as the poly(NIPAM-co-AAc) hydrogels in the present study displayed higher storage moduli values and exhibited higher degrees of crosslinking (figure 4.1.2) compared to Wisniewska et.al [45].

4.1.3 PGSE NMR

Three poly(NIPAM-co-AAc) hydrogels were swollen in β-cyclodextrin, which was used as a probe, and analysed using pulsed gradient spin-echo (PGSE) NMR. The diffusion coefficient of the probe molecule was measured in D_2O solution and subsequently within the hydrogel network. Due to higher fractal resistance and tortuosity, the diffusion of probe molecules in a hydrogel network is slower than the diffusion in D_2O solution [45]. By comparing the two diffusion coefficients of the probe molecule, and by using the equation models presented in section 2.4.2, the mesh sizes of the parallels could be obtained. Furthermore, the hydrogels were all of the same formulation so that reproducibility of the hydrogels' microstructure could be investigated. Hydrogel formulation is described in section 3.2.1.

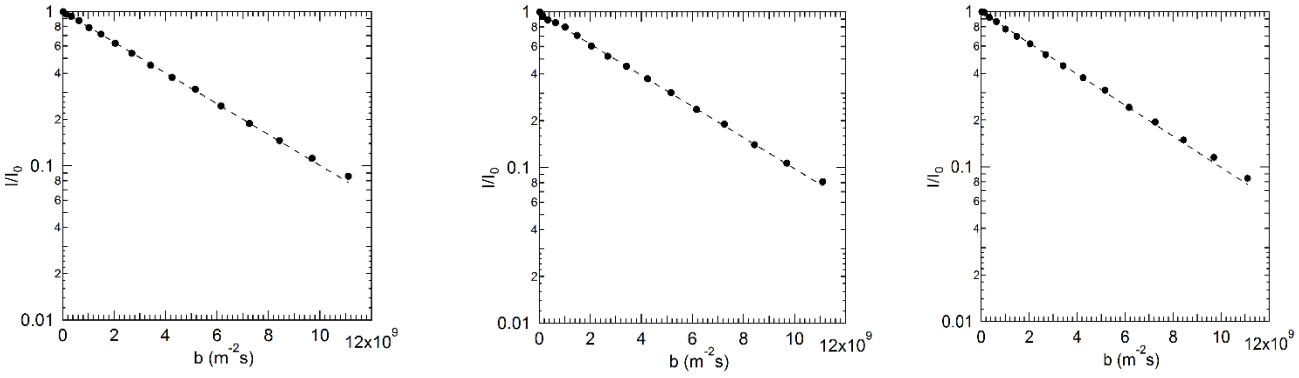

Figure 4.1.7: Normalised echo attenuations for the diffusion of the -CH_2 group of β-cyclodextrin in poly(NIPAM-co-AAc) hydrogels 1-3 (from left to right), where $b = \gamma^2 g^2 \delta^2 (\Delta - \frac{\delta}{3})$.

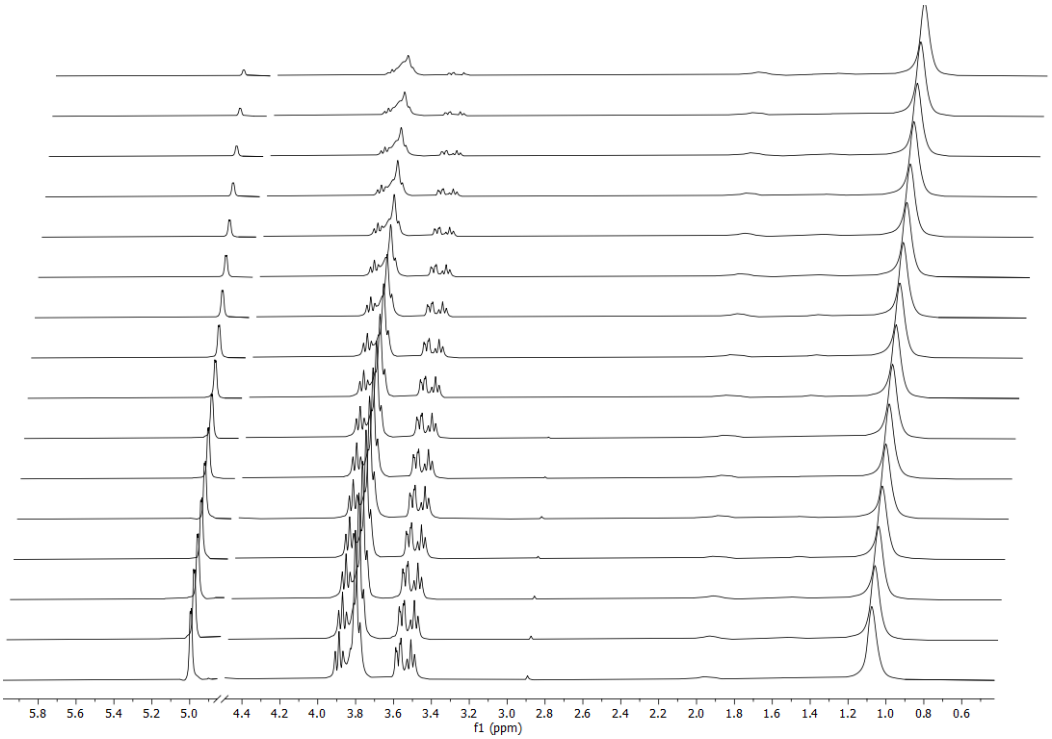

Figure 4.1.8: [1]HNMR signal decay for β-cyclodextrin in poly(NIPAM-co-AAc) hydrogel.

Three peaks of β-cyclodextrin do not overlap with poly(NIPAM-co-AAc) hydrogel and are used for analysis. The peaks are assigned to the chemical shift of -CH_2 groups (3,9 and 3,5 ppm) and -OH (5 ppm)

The size of β-cyclodextrin was determined by measuring probe diffusion in D2O. Table 4.1.5 displays the diffusion coefficient of β-cyclodextrin in pure D_2O that was obtained by fitting eq. (8) to NMR data. The corresponding hydrodynamic radii of β-cyclodextrin was calculated using eq. (13).

Table 4.1.5: Diffusion coefficient and hydrodynamic radii of β-cyclodextrin

$\boldsymbol{D_0 * 10^{10}\ m^2\ s^{-1}}$	$\boldsymbol{r_s(nm)}$
$\boldsymbol{2,6 \pm 0,02}$	$0,77 \pm 0,02$

A study of cyclodextrin molecules hydrodynamic properties in dilute solutions by Pavlov et.al [91] found the hydrodynamic radii of β-cyclodextrin in H_2O to be 0,77 nm. The translational diffusion coefficient in the same medium was studied using a Tsvetkov polarizing diffusiometer and found by Pavlov to be $2,9 * 10^{-10} m^2\ s^1$. The value of the hydrodynamic radii is based on mathematical models and might differ from the size of the real molecule. Furthermore, the difference in characterization methods between the present study and

Pavlov, regarding diffusion coefficient, does carry some uncertainty when comparing the two values. Nevertheless, the results seem to be in line with literature.

The mesh sizes of the poly(NIPAM-co-AAc) hydrogels were obtained by using eq. (14) and are presented in table 4.1.6, along with the diffusion coefficients of β-cyclodextrin in the respective hydrogels.

Table 4.1.6: Diffusion coefficient of β-cyclodextrin in poly(NIPAM-co-AAc) hydrogel (D_g), the diffusion quotient ($\frac{D_g}{D_0}$), and mesh size (ξ^{NMR}). The three hydrogels are parallels of the same formulation (see section 3.2.1)

Poly(NIPAM-co-AAc) hydrogel	$\boldsymbol{D_g * 10^{10}\ m^2\ s^{-1}}$	$\boldsymbol{\frac{D_g}{D_0}}$	$\boldsymbol{\xi^{NMR}}$ **(nm)**
1	$2{,}30 \pm 0{,}016$	0,88	6,15
2	$2{,}31 \pm 0{,}032$	0,89	6,28
3	$2{,}31 \pm 0{,}028$	0,89	6,47
average	$\mathbf{2,31 \pm 0,045}$	**0,89**	$\mathbf{6{,}3 \pm 0{,}2}$

The mesh sizes obtained through PGSE NMR studies are relatively small compared to the mesh sizes obtained through rheological analysis and dynamic swelling studies for the same system. The average mesh sizes obtained through swelling and rheological analysis were $10{,}1 \pm 0{,}2$ and $9{,}6 \pm 0{,}1$ nm, respectively. One reason for the disparity in mesh sizes could be the different methods of calculation. The PGSE NMR is susceptible to heterogeneity in samples [82] and the poly(NIPAM-AAc) hydrogel network is inhomogeneous due to varying density of polymer regions [40, 47]. Whether the density variations are comprehensive enough to have a significant impact on the NMR analysis is unclear.

It would perhaps be more pertinent to compare the obtained mesh sizes with results in literature [45], obtained by the same method for a comparable system. For the same poly(NIPAM-co-AAc) hydrogel formulation, Wisniewska et.al [45] found the average mesh size to be $9{,}6 \pm 0{,}2$ nm, based on the diffusion quotients of five dextrans (probe molecule) with varying molecular weights. The smallest probe molecule used in the study of Wisniewska was 5 kDa dextran, with a hydrodynamic radius of 1,6 nm, which is approximately twice the size of the β-cyclodextrin molecule used in the present study. One of the limitations of probe diffusion experiments is that they are quite sensitive to the size of the

probe molecules [83]. Therefore, it is possible that the size of the β-cyclodextrin probe is too small to accurately detect the mesh size.

4.2 Self-assembling chitosan hydrogel

The self-assembling chitosan (SA-CS) hydrogel was synthesized by modifying the chitosan polymer with either thioglycolic acid or 4-maleimidobutyric acid. Polymer-polymer conjugation was achieved through Michael addition by mixing of the two modified polymers. The hydrogel was characterized by oscillatory rheological measurements, dynamic swelling and PGSE NMR studies.

4.2.1 Rheology and swelling studies

The linear viscoelastic region (LVE region) of self-assembling chitosan hydrogel (SA-CS) was determined by amplitude sweep measurement at a constant frequency of 1 Hz (figure 4.2.1). From the amplitude sweep data the LVE region was determined to lie within $\gamma<10\%$.

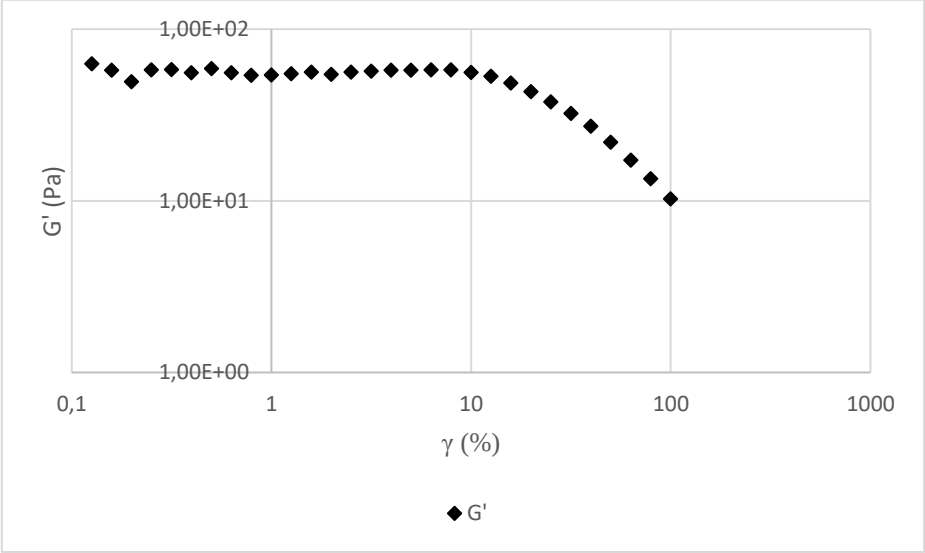

Figure 4.2.1: Characterization of the storage modulus (G') as a function of shear strain (γ) for SA-CS hydrogel. Frequency was fixed at 1 Hz

Once the LVE region of the hydrogel had been determined, frequency sweep measurements were performed at a constant shear strain of 1% (figure 4.2.2).

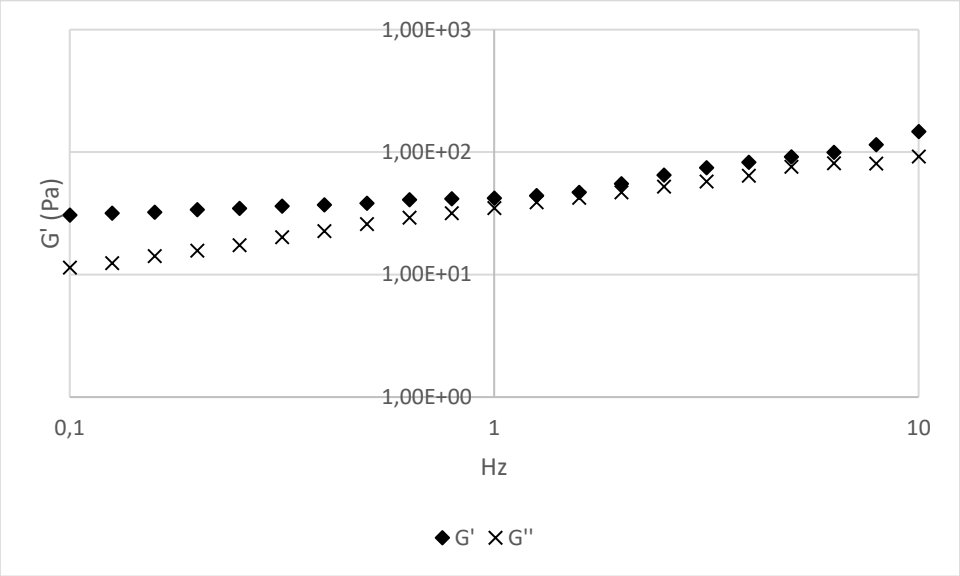

Figure 4.2.2: Characterization of the storage modulus (G') and loss modulus (G'') as a function of frequency (Hz) for SA-CS hydrogel. Shear strain was fixed at 1%

The storage modulus (G') of SA-CS seem to exhibit frequency dependent behaviour. At frequencies >1 Hz, this behaviour becomes more apparent. The viscoelastic behaviour of chitosan is determined by the degree of crosslinking [61]. It is possible that the degree of covalent crosslinking is too small, and that the storage moduli values displayed in figure 4.2.2 derive from physical entanglements formed by chitosan chains. Also, both the storage modulus (G') and the loss modulus (G'') increase with frequency, without reaching a crossover point, which is in line with results found in literature for a chemically crosslinked network which is "dissolved" in a second physical network of entanglements [61]. An entangled chitosan network can be formed by dissolving chitosan in an acidic aqueous medium [33]. It is also possible that covalent crosslinking did not occur at all. At any rate, the low storage moduli values and the frequency dependent behaviour suggests that the SA-CS hydrogel network consists of physical crosslinks, and not permanent covalent crosslinks.

Swelling analysis (section 3.3.2) of the SA-CS hydrogel was performed at the initial state. In the present study, the initial state is defined as the state of the system 24 hours after the mixing of thiolated chitosan with chitosan modified by maleimide coupling. At the initial state, a weak gel had been formed, as indicated by the rheological analysis in figure 4.2.2. The

swelling behaviour of the gel at the initial state further implied the absence of a permanent hydrogel network. Rather than displaying swelling behaviour, the gel semi-dissolved in its aqueous surroundings. The dissolution occurred in a matter of a few days. As the entangled chitosan hydrogel is characterized by weak mechanical strength and a tendency to dissolve [33], it seems likely that entangled chitosan was formed rather than covalently crosslinked chitosan.

Whilst preparing SA-CS samples for NMR measurements, a visible increase in the volume of the gels was observed as they were incubated in β-cyclodextrin. As no H_2O should be present in the networks of the gels when analysed by NMR, the gels had been freeze-dried a second time after being formed. To investigate this behaviour, a second synthesis of SA-CS was initiated. The sample was freeze-dried after it had been formed at the initial state. The dry weight was recorded, and the hydrogel was incubated in milli Q for 1 week.

Table 4.2.1: Dry weight (W_d), saturated weight (W_s), mass swelling ratio (Q_m), and water content (W_c) of SA-CS hydrogel incubated in milli Q water for 1 week.

W_d (g)	W_s (g)	Q_m	W_c (%)
0,0917	4,2907	46,8	4679

As the "discovery" of the swelling ability of SA-CS occurred quite late in the present study, and due to expensive chemicals, time-consuming synthesis, and a limited timetable, only one parallel of swollen SA-CS hydrogel was produced

After 1 week of incubation in milli Q, it was clear that the lyophilized SA-CS hydrogel had swollen, and a mass swelling ratio of 46,8 was obtained. Further measurements were performed, but the gel had seemingly reached an equilibrium, as the weight did not increase beyond this time. Freeze-drying the sample produced a material with a white colouring and a sponge-like feel at the dry state. The hydrogel was incubated in milli Q for two weeks, at which point it was used for rheological analysis (figure 4.2.3). The gel did not appear to undergo any form of dissolution within this time.

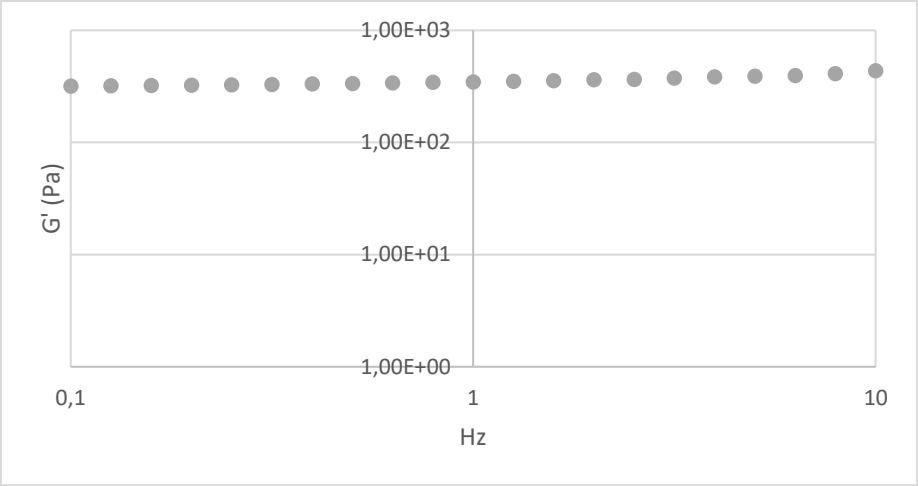

Figure 4.2.3: Characterization of the storage modulus (G') as a function of frequency (Hz) for swollen SA-CS hydrogel. Shear strain was fixed at 1%

When comparing the results in figures 4.2.2 and 4.2.3, the differences must be stated first. The hydrogel in figure 4.2.3 was freeze-dried after mixing of the modified polymers, and frequency sweep measurement was performed in a swollen state. The hydrogel presented in figure 4.2.2 was not lyophilized after mixing of the modified polymers, and frequency sweep measurement was performed at the initial state. The syntheses are independent and was performed at different times. The chemical composition of the gels is the same.

The swollen SA-CS in figure 4.2.3 shows almost no dependence with frequency. Furthermore, the average storage moduli values are larger by a factor of 6, compared to figure 4.2.2. Due to the high water content of a swollen gel, we would expect it to be less mechanically strong, compared to a gel at the initial state. Lyophilization affects the pore structure of hydrogels and may have contributed to the increase in swelling ability. However, the major differences between parallels suggests that covalent crosslinking only occurred in the second synthesis. Further investigation into this matter is needed to provide conclusive results.

4.2.2 PGSE NMR

The diffusion coefficient of the probe molecule, β-cyclodextrin was measured in D2O and in SA-CS hydrogel, respectively, and subsequently used to obtain the mesh size of SA-CS hydrogel

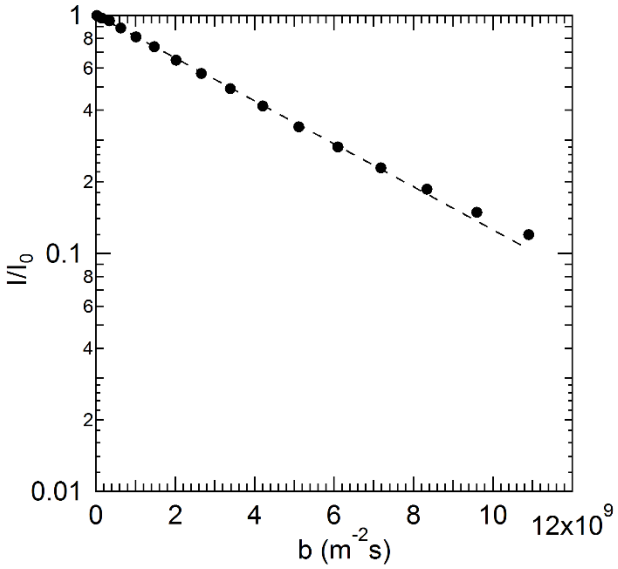

Figure 4.2.4: Normalised echo attenuations for the -CH_2 group of β-cyclodextrin in self-assembling chitosan hydrogel, where $b = y^2 g^2 \delta^2 (\Delta - \frac{\delta}{3})$.

The diffusion-coefficient of β-cyclodextrin was obtained by fitting NMR data to eq. (8), the corresponding hydrodynamic radii was obtained by using eq. (13).

Table 4.2.2: Diffusion coefficients of β-cyclodextrin in aqueous solution (D_0) and the corresponding hydrodynamic radii (r_s)

$\boldsymbol{D_0 * 10^{10}\ m^2\ s^{-1}}$	$\boldsymbol{r_s\ (nm)}$
$2{,}6 \pm 0{,}02$	$0{,}77 \pm 0{,}02$

As previously discussed (see section 4.1.3) the diffusion coefficient and corresponding hydrodynamic radius of β-cyclodextrin seem to be in line with values found in literature [91]. The mesh size of SA-CS was obtained by using eq. (14) and is presented in table 4.2.3 along with the diffusion quotient and the diffusion coefficient of β-cyclodextrin in SA-CS hydrogel.

Table 4.2.3: Diffusion coefficient of β-cyclodextrin in SA-CS (D_g), diffusion quotient (D_g/D_0) and mesh size of SA-CS (ζ^{NMR})

$D_g * 10^{10}\ m^2\ s^{-1}$	$\frac{D_g}{D_0}$	$\zeta^{NMR}\ (nm)$
$2{,}08 \pm 0{,}02$	0,84	4,1

The mesh size of SA-CS was found to be 4,1 nm, which is quite small considering most natural polymer hydrogels have mesh sizes in the range of 5-100 nm [92]. As discussed in section 4.1.3, the probe diffusion experiments sensitivity to the size of probe molecules [83] and the small size of the probe used in the present study, can possibly lead to the mesh size of SA-CS not being detected accurately. Furthermore, a very small mesh size could suggest a high degree of crosslinking of the hydrogel network [15], based on the storage modulus of SA-CS (figures 4.2.2 and 4.2.3), this seems unlikely.

4.3 Chitosan hydrogel

Chitosan hydrogels were synthesized with different concentrations of crosslinker. The gels were characterized by oscillatory rheological measurements and swelling. An overview of crosslinker concentration in the samples is given in table 4.3.

Table 4.3: Crosslinker concentration in chitosan hydrogel samples 1-8. M refers to molar concentration

Sample	Glutaraldehyde (% v/v)	Na_2SO_4 solution (M)
C1	0,74	0,05
C2	0,74	0,04
C3	0,8	0,05
C4	0,8	0,04
C5	0,074	0,05
C6	0,074	0,04
C7	0,08	0,05
C8	0,08	0,04

4.3.1 Rheology

An amplitude sweep was carried out on each sample (figure 4.3.1), and the LVE region was determined to lie within the range of $\gamma < 10\%$.

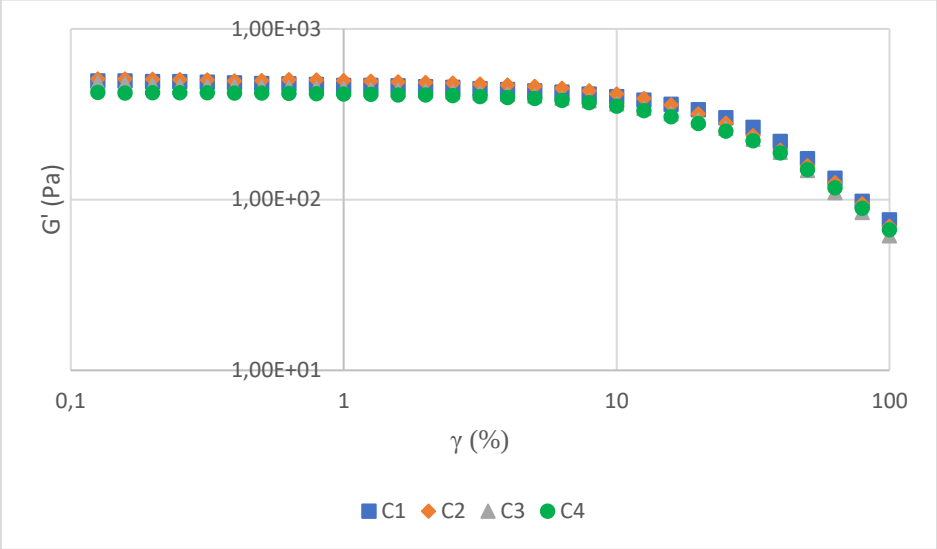

Figure 4.3.1: Characterization of storage modulus (G') as a function of shear strain for chitosan hydrogel samples 1-4 with different concentrations of crosslinker. The frequency was fixed at 1 Hz for all samples

For the subsequent frequency sweep measurements (figures 4.3.2 and 4.3.3) the shear strain was fixed at 1% as it suited all samples.

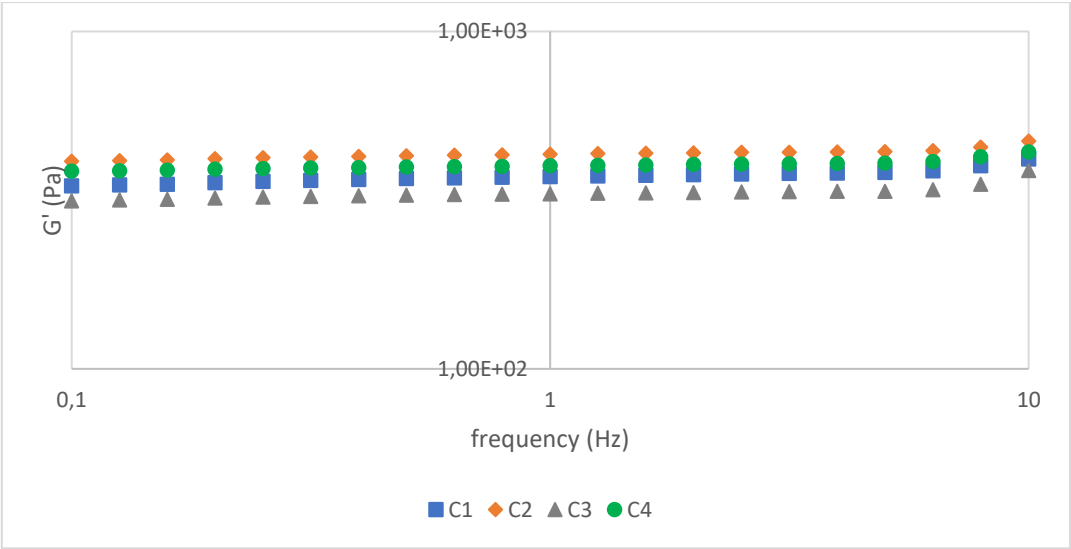

Figure 4.3.2: Characterization of the storage modulus as a function of frequency for chitosan hydrogels synthesized with different amount of crosslinker. Strain was fixed at 1%. The formatting of the Y-axis was designed so that the difference in samples could be observed more easily

The frequency sweep measurement showed that the storage moduli (G') was mostly independent of frequency for all chitosan hydrogel samples. The samples displayed gel-like behaviour irrespective of crosslinker concentration. Interestingly, it appears to be a link between mechanical strength and amount of sodium sulfate. The two samples containing 0,05 $mol * L^{-1}$ Na_2SO_4 solution displayed the lowest G' values, whilst the samples containing 0,04 $mol * L^{-1}$ Na_2SO_4 solution displayed the highest. The goal of using sodium sulfate as a co-crosslinker is for it to partially replace glutaraldehyde to reduce the toxicity of the hydrogels. Due to sodium sulfate being an ionic crosslinker, we expect the hydrogels to be partially physically crosslinked and therefore exhibit less mechanical strength. The trend observed in figure 4.3.2 clearly indicates that sodium sulfate contributes in the crosslinking of the hydrogels.

When we study the storage moduli of the samples containing 1/10 of the amount of glutaraldehyde compared to samples C1-C4, and the connection between G' values and sodium sulfate concentration, the opposite trend is observed (figure 4.3.3).

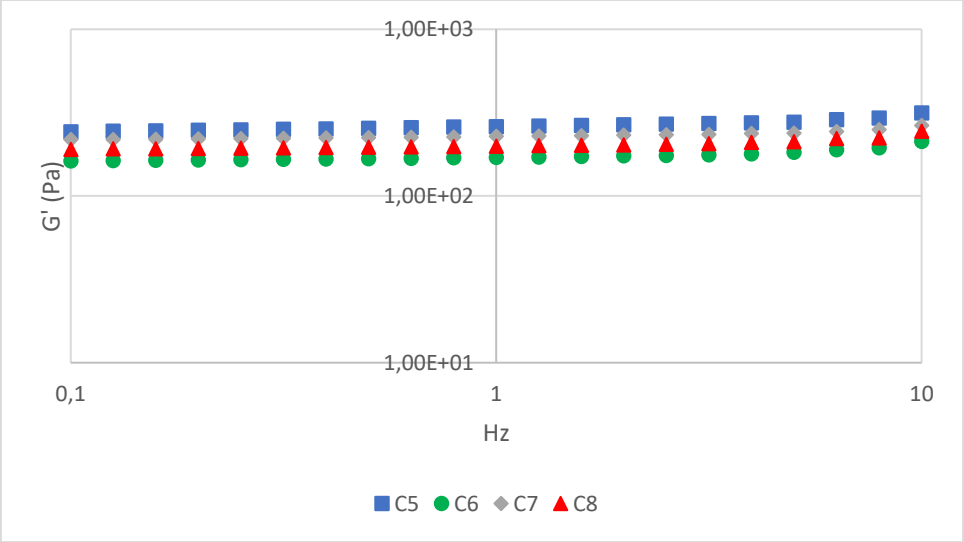

Figure 4.3.3: Characterization of the storage modulus as a function of frequency for chitosan hydrogels. The samples C5-C8 differ in crosslinker concentration.

Chitosan hydrogel samples C5-C8 differ from the samples C1-C4 in that they contain a significantly reduced amount of glutaraldehyde (see table 4.3). Nevertheless, the storage moduli values are independent of frequency, indicating crosslinked polymer networks and gel-like behaviour. Another interesting difference is the connection between G' values and sodium sulfate concentration. In figure 4.3.3, the samples with the highest concentration of

sodium sulfate solution displays the largest storage moduli (G') values, which is the opposite of the trend observed in figure 4.3.2. A likely explanation could be that the glutaraldehyde concentration is so small in the samples C5-C8, that the large majority of crosslinks in the hydrogel network stem from sodium sulfate. Therefore, it would make sense that samples with higher concentration of sodium sulfate are more densely crosslinked. Furthermore, the storage moduli values in figure 4.3.3 are 80% lower on average compared to the values in figure 4.3.2. Physically crosslinked hydrogels are less mechanically strong than permanent hydrogels, so this is an expected result.

It is also possible that the hydrogel samples C5-C8 are covalently crosslinked by glutaraldehyde, and that the reduced storage moduli values are solely a result of the reduced concentration of glutaraldehyde, though the opposite trend between sodium sulfate concentration and storage moduli values in the two measurements seem to indicate otherwise.

4.3.2 Swelling studies

Although the chitosan gels displayed reasonable mechanical properties when characterized by oscillatory measurements, the swelling studies were challenging. Potential swelling was studied at both the initial state and from a dry state as a result of lyophilization. Regarding studies at the initial state, samples were incubated in water between 24-48 hours after synthesis and left undisturbed for one week. After this period, periodical measurements were initiated to investigate any potential increase in weight. During these measurements, it proved difficult to separate the samples from the aqueous media. This was due to the samples seemingly undergoing partial dissolution in water. Some swelling data was recorded, but the risk of non-discarded water causing the increase in weight is significant. Results are therefore not presented in the present study. The dissolution tendencies indicate a reversible gel network.

Regarding studies at the dry state, lyophilized samples were incubated in water and subsequently treated in the same manner as gels at the initial state. Unlike gels at the initial state, the lyophilized gels did not dissolve in water, but rather turned into a sponge like material with an orange colouring, as seen in figure 4.3.4. However, the samples did not display any swelling ability.

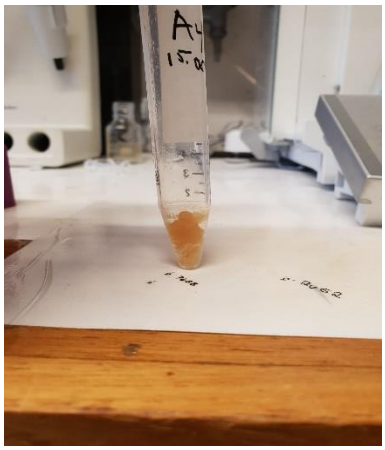

Figure 4.3.4: Lyophilized chitosan hydrogel after one week of incubation in water.

As a note, swelling studies were only performed on parallels of samples C1-C4.

4.4 Gelatin hydrogel

Gelatin samples were synthesized with different concentrations of crosslinker. An overview of crosslinker concentration in the samples is given in table 4.4.

Table 4.4: Samples of gelatin were synthesized with different concentration of crosslinker

Sample	Glutaraldehyde (% v/v)	Na_2SO_4 solution $(mol * L^{-1})$
G1	0,74	0,05
G2	0,74	0,04
G3	0,8	0,05
G4	0,8	0,04

4.4.1 Rheology

An amplitude sweep was performed to determine the LVE region of the gelatin sample (figure 4.4.1). Storage modulus values were inconsistent and the determination of the LVE region could not be performed with certainty.

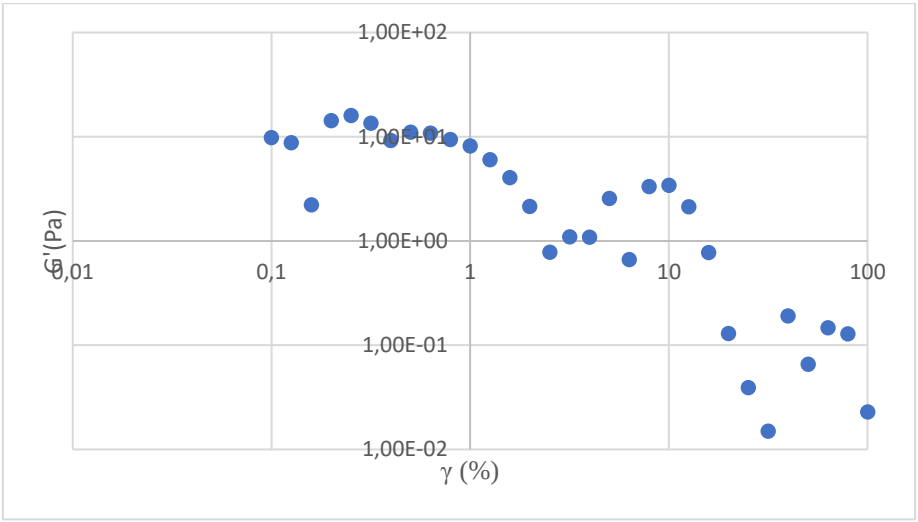

Figure 4.4.1: Characterization of storage modulus (G') as a function of shear strain (γ) for gelatin. The frequency was fixed at 1 Hz

Subsequently, a frequency sweep measurement was attempted (figure 4.4.2). The shear strain was set at 0,1%.

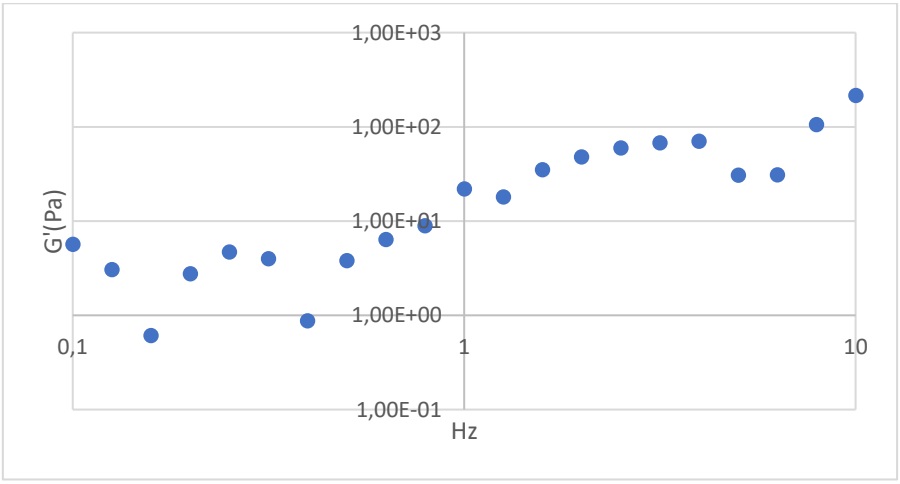

Figure 4.4.2: Characterization of the storage modulus (G') as a function of frequency (Hz) for gelatin. The shear strain was fixed at 1%

The gelatin sample seemed to exhibit frequency dependent behaviour, but the behaviour was not consistent. Based on the frequency sweep measurement, it is clear that gelatin did not form a gel. The gelatin polymer solution displayed quite low viscosity compared to the chitosan polymer solution. The rheological measurements for both systems were performed by using a parallel-plate measuring system with 2mm gap between geometries. These parameters were used for the gelatin system in order to produce results that were comparable with the chitosan and chitosan-gelatin systems. Considering the low viscosity of the gelatin system, it is possible that this gap height was too large, and consequently caused the result presented in figure 4.4.2.

4.4.2 Swelling studies

Similar to chitosan, swelling studies of the gelatin system proved difficult. Measurements did not provide any evidence of a hydrogel being formed. The samples fully dissolved in the aqueous media, and separation of the sample and water was impossible.

4.5 Chitosan-gelatin hydrogel

Three systems of chitosan-gelatin (CG) hydrogels were synthesized with different concentrations of crosslinker. Table 4.5 and 4.6 provide an overview of the systems and crosslinker concentrations, respectively, that was studied in this thesis. The hydrogels were characterized by rheological oscillatory measurements and swelling.

Table 4.5: Overview of the three systems of chitosan-gelatin hydrogel that was studied. P is the amount of polymer, referred to percentage of mass per volume, in the samples, C:G is the ratio of chitosan and gelatin referred to mass, and T is the temperature at which the solutions were rested before addition of Na_2SO_4 solution

System	P (% w/v)	C:G (g)	T (°C)
X	2,5	4,5 : 1	50
Y	1	1 : 1	50
Z	1	1: 1	22

Table 4.6: Six hydrogels were synthesized with different concentrations of crosslinkers glutaraldehyde and sodium sulfate. Samples 5 and 6 were used as control samples

Sample	Glutaraldehyde (% v/v)	Na_2SO_4 solution ($mol * L^{-1}$)
1	0,74	0,05
2	0,74	0,04
3	0,8	0,05
4	0,8	0,04

4.5.1 Rheology

An amplitude sweep measurement was performed on hydrogel system Z to determine the LVE region (figure 4.5.1). The LVE region was determined to lie within $\gamma < 10\%$.

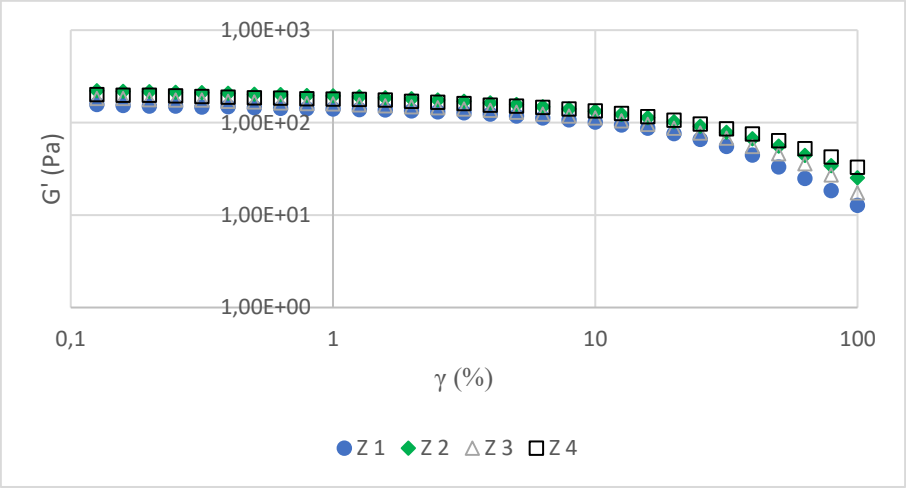

Figure 4.5.1: Storage moduli as a function of strain (γ) for CG hydrogel system Z. Frequency was fixed at 1 Hz. Samples 1-4 vary in concentration of crosslinkers glutaraldehyde and sodium sulfate

Subsequent frequency sweep measurements were performed with strain (γ) fixed at 1%. This was constant for all three CG hydrogel systems, as we expect the LVE region to be roughly the same. Frequency sweep measurements of CG hydrogel systems X, Y and Z are presented in figures 4.5.2, 4.5.3 and 4.5.4, respectively.

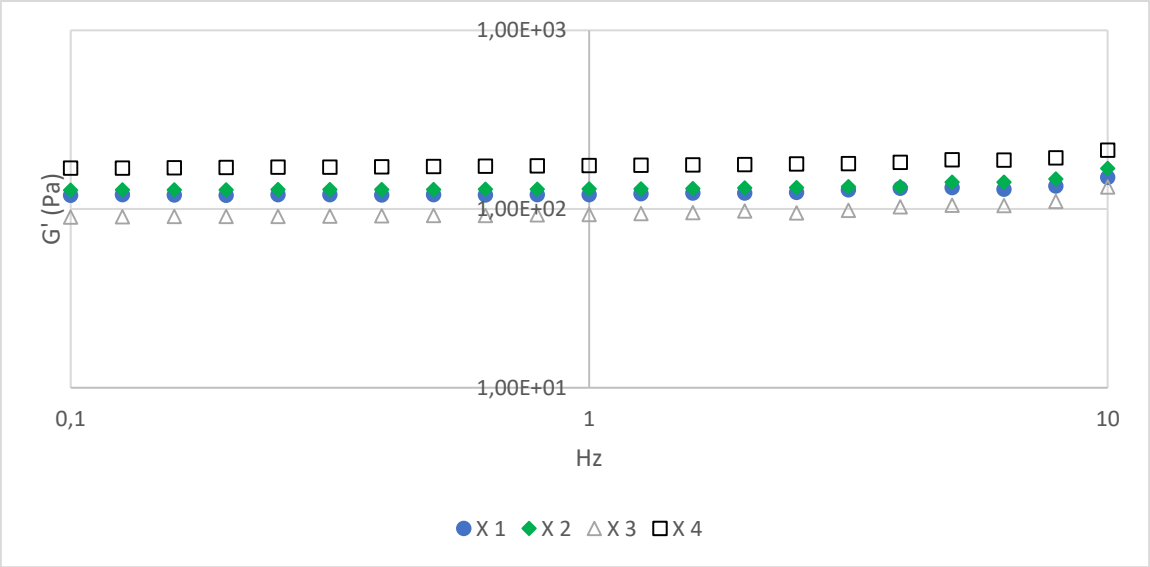

Figure 4.5.2: Characterization of the storage moduli as a function of frequency for CG hydrogel system X. Samples 1-4 vary in concentration of crosslinkers glutaraldehyde and sodium sulfate. Strain was fixed at 1%

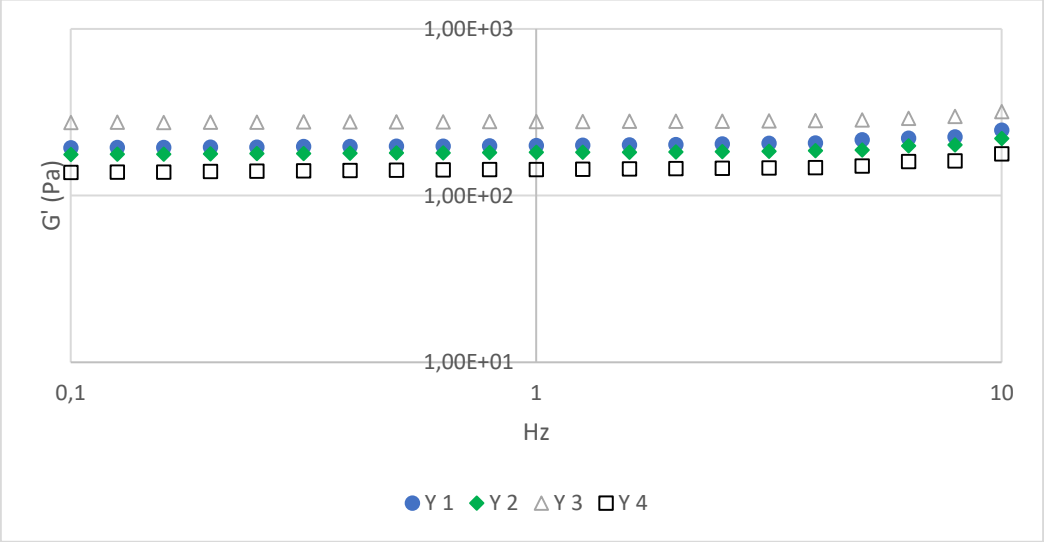

Figure 4.5.3: Characterization of the storage modulus as a function of frequency for CG hydrogel system Y. Samples 1-4 vary in concentration of crosslinkers glutaraldehyde and sodium sulfate. Strain was fixed at 1%

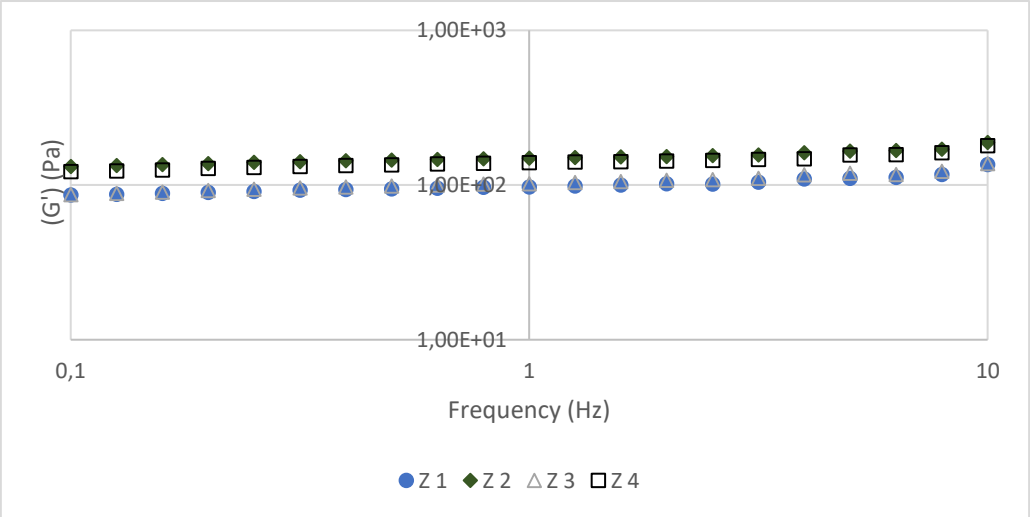

Figure 4.5.4: Characterization of the storage modulus as a function of frequency for CG hydrogel system Z. Sample 1-4 vary in concentration of crosslinkers glutaraldehyde and sodium sulfate. Strain was fixed at 1%

All systems displayed frequency independent behaviour across the frequency interval, indicating that gels are formed for all three systems, independent of crosslinker concentration. Interestingly, no clear trend between concentration of crosslinkers and the storage modulus can be deducted from the three figures. Covalently crosslinked hydrogels display better mechanical properties than hydrogels that are physically crosslinked, and higher degree of crosslinking leads to stronger hydrogels [28, 32]. Therefore, we would expect the sample with the highest concentration of glutaraldehyde and lowest concentration of sodium sulfate i.e. sample 4, to display the largest storage modulus values.

Unexpectedly, this is only the case for CG system X. Furthermore, sample 4 displays the lowest G' values in CG system Y, which could indicate that formulation of the systems i.e. ratio between polymers and temperature are more important factors for the mechanical properties of the gels. This is something that could merit further investigation. Also, the reproducibility of the systems is a factor that could have contributed to the unexpected results. Oscillatory rheological analysis of hydrogels presented some challenges. With the aim of comparing the rheological data of different hydrogels, it was desirable to maintain as consistent parameters of analysis as possible. Hydrogels are dynamic systems, and their mechanical properties can vary significantly based on method of synthesis and the chemicals that are used. This was the case for chitosan-gelatin hydrogels, where the varying amounts of glutaraldehyde and sodium sulfate had an impact on the viscosity of the products. Firstly, separation of product from Na_2SO_4 solution, and secondly, oscillatory analysis using the parallel-plate measuring system and a 2 mm gap height, proved to be difficult due to some

samples displaying low viscosity. It is likely that these challenges have been reflected in the rheological results.

We compared the average storage modulus at 1 Hz for the three CG hydrogel systems and chitosan hydrogel (presented in section 4.3 and figure 4.3.2) in table 4.5.1.

Table 4.5.1: A comparison of the storage modulus for four hydrogel systems. The storage modulus (G') is presented as the average value at 1 Hz for all samples (1-4) of each different system

System	G' (Pa)
CG hydrogel X	130
CG hydrogel Y	201
CG hydrogel Z	122
Chitosan hydrogel	384

The gel formulated from chitosan as a sole polymer, clearly exhibited the largest mechanical strength. Hydrogen bonds are formed between gelatin and chitosan in CG hydrogel [65]. It is likely that the low mechanical strength of gelatin have contributed to the overall reduction in mechanical strength of CG hydrogels compared to chitosan hydrogel. Furthermore, the hydrogen bonds stem from interactions between the amino groups in chitosan and residues of glutamate and aspartic acids in gelatin. Glutaraldehyde reacts with the same amino groups in the crosslinking reaction. Less available amino groups could influence the mechanical strength.

Out of the three CG hydrogel systems we should therefore expect CG hydrogel X to display the largest storage moduli values, as the ratio between chitosan and gelatin is 95-5, referred to weight. As this is not the case, it is possible that the relationship between gel strength and chitosan-gelatin ratio is not as linear as expected. Another possibility is that the experimental difficulties that was encountered, have contributed to unstable measurements.

4.5.2 Swelling studies

Swelling was not recorded for any of the CG hydrogel systems. The samples exhibited the same behaviour as chitosan gels (see section 4.3.2) both at the initial and lyophilized state. In an effort to improve the swelling ability, pre-freezing (see section 3.3.4) was performed on CG system Z. The samples were stored at -18 °C for 24 hours before lyophilization. No apparent improvement was detected in the aftermath of this method.

5 Summary and conclusions

Poly(NIPAM-co-AAc) hydrogels were successfully synthesized by chemical crosslinking and the use of initiators. The hydrogels exhibited good mechanical strength and excellent swelling ability. Oscillatory rheological measurements revealed relatively large storage moduli values compared with similar hydrogel formulations in literature, thus indicating a high degree of crosslinking. Gelation occurred within one hour of synthesis, and polymerization of the hydrogel network was ongoing at least seven hours after synthesis. Dynamic swelling studies showed a clear trend between ratio of initiators (TEMED and APS) and mass swelling ratio. Increasing the TEMED to APS ratio from 8 :9 to 9 : 1, lead to a near 2-fold increase in mass swelling ratios. By using pulsed gradient spin-echo NMR experiments, an average mesh size for poly(NIPAM-co-AAc) hydrogels was found to be 6,3 nm. The relatively small mesh size is believed to stem from using β-cyclodextrin as the probe. It is possible that the β-cyclodextrin molecule is too small to accurately detect the hydrogel mesh size.

Self-assembling chitosan hydrogel was synthesized through Michael addition, and provided mixed results. At first, the hydrogel did not show signs of covalent crosslinking. Oscillatory rheological measurements indicated a weak gel displaying frequency dependent behaviour. The SA-CS network seemed to consist of chitosan entanglements. Lack of swelling ability and a tendency to dissolve in aqueous media at the initial state, strengthened this assumption. A second synthesis, in which the sample was lyophilized at the initial state, exhibited far greater properties. A mass swelling ratio of 47 was obtained after lyophilization. Oscillatory rheological measurement on the swollen SA-CS indicated a stronger and frequency independent hydrogel. The mesh size was found to be 4,1 nm. Common to poly(NIPAM-co-AAc) hydrogel, it is believed that the small hydrodynamic radius of the probe, led to mesh sizes not being accurately detected. It is possible that the first synthesis was unsuccessful, and that covalent crosslinking was either inadequate, or did not materialise. The porous structure which is created by lyophilization, may have contributed to the improved swelling that was observed in the second synthesis.

Chitosan was used as the sole gel-forming polymer and co-crosslinked by glutaraldehyde and sodium sulfate solution, to decrease potential toxicity. The system displayed gel-like behaviour i.e. frequency independent storage modulus, when analysed by oscillatory rheological measurements. The introduction of sodium sulfate as a co-crosslinker was shown to affect the mechanical properties of the gel, indicating a partially ionically crosslinked

network. Mass swelling ratio of chitosan gel was not obtained as the gel showed little proof of swelling. Dissolution of the gel was observed, indicating a reversible network.

Gelatin polymer was co-crosslinked by glutaraldehyde and sodium sulfate solution. The system did not display gel-like behaviour when analysed by oscillatory rheological measurements, nor dynamic swelling. Crosslinking of gelatin polymer by glutaraldehyde, seemingly had little effect. The liquid state of the system made the separation of samples from sodium sulfate solution nearly impossible. This led to experimental difficulties when attempting rheological analysis. It is likely that these difficulties affected the results.

A co-polymer system of chitosan and gelatin (CG) was synthesized and co-crosslinked by glutaraldehyde and sodium sulfate solution. Three systems were synthesized with varying polymer concentration, weight ratio of chitosan and gelatin, and temperature. Oscillatory rheological measurements showed that all systems were independent of frequency, thus displaying gel-like behaviour. Measurements indicated that the introduction of gelatin as a co-polymer, reduced the mechanical strength of the systems, compared to chitosan gels. Furthermore, the expected relationships between storage modulus and glutaraldehyde concentration, and storage modulus and chitosan concentration were not observed. This could indicate a non-linear relationship between these factors. Though, it is suspected that difficulties regarding the rheological measuring system and sample viscosity influenced the results.

Comparing the different hydrogels, poly(NIPAM-co-AAc) hydrogel exhibited superior swelling ability and mechanical properties. The chitosan-gelatin hydrogels showed gel-like behaviour based on rheological results, but dissolution tendencies and a lack of swelling ability indicate that they are poor alternatives to poly(NIPAM-co-AAc) hydrogels. The mixed results from the syntheses of SA-CS hydrogel warrants further investigation. However, one parallel displayed good mechanical strength, stability against dissolution, and swelling ability. The SA-CS hydrogel could provide a reasonable, biocompatible alternative to synthetic hydrogels in the future.

6 Further work

Further research can be pursued to gain a better understanding of hydrogels. Further investigation into some of the results presented in the present study could facilitate more effective syntheses in the future. A more comprehensive study of the relationship between the initiator couple TEMED/APS and the gelation and swelling of poly(NIPAM-co-AAc) hydrogel, could be beneficial for controlling the mass swelling ratio of the product in a more accurate way. Also, studying the potential impact on hydrogel swelling by varying the concentrations of each initiator whilst keeping the ratio fixed, could prove an interesting study.

The SA-CS hydrogel showed signs of being a promising alternative to synthetic hydrogels. Further studies of the system to provide conclusive results is needed. Such studies could include investigating the impact of varying weight ratios between the two modified polymers. This would facilitate a better understanding of the crosslinking reaction. Assuming an ideal ratio of 1 : 1, this study could also yield valuable information about how far the ratio could deviate from the ideal, without being detrimental to the covalent crosslinking reaction

7 Bibliography

1. Zhang, X.-Z. and C.-C. Chu, *Synthesis of temperature sensitive PNIPAAm cryogels in organic solvent with improved properties.* Journal of Materials Chemistry, 2003. **13**(10): p. 2457-2464.
2. Ji Yin, Y., et al., *Preparation and characterization of hydroxyapatite/chitosan–gelatin network composite.* Journal of Applied Polymer Science, 2000. **77**(13): p. 2929-2938.
3. Billard, A., et al., *Liposome-loaded chitosan physical hydrogel: Toward a promising delayed-release biosystem.* Carbohydrate Polymers, 2015. **115**: p. 651-657.
4. Li, X., et al., *A PNIPAAm-based thermosensitive hydrogel containing SWCNTs for stem cell transplantation in myocardial repair.* Biomaterials, 2014. **35**(22): p. 5679-5688.
5. P.T. Sudheesh Kumar, S.A., K. Manzoor, S.V. Nair, H. Tamura, R. Jayakumar, *Preparation and characterization of novel β-chitin/nanosilver composite scaffolds for wound dressing applications.* Carbohydrate Polymers, 2010. **80**(3): p. 761-767.
6. Snowden, M.J., et al., *Colloidal copolymer microgels of N -isopropylacrylamide and acrylic acid: pH, ionic strength and temperature effects.* Journal of the Chemical Society, Faraday Transactions, 1996. **92**(24): p. 5013-5016.
7. Denisin, A.K. and B.L. Pruitt, *Tuning the Range of Polyacrylamide Gel Stiffness for Mechanobiology Applications.* ACS applied materials & interfaces, 2016. **8**(34): p. 21893.
8. Dong, L.-C. and A.S. Hoffman, *Synthesis and application of thermally reversible heterogels for drug delivery.* Journal of Controlled Release, 1990. **13**(1): p. 21-31.
9. Hamidi, M., A. Azadi, and P. Rafiei, *Hydrogel nanoparticles in drug delivery.* Advanced Drug Delivery Reviews, 2008. **60**(15): p. 1638-1649.
10. Rathna, G., *Gelatin hydrogels: enhanced biocompatibility, drug release and cell viability.* Official Journal of the European Society for Biomaterials, 2008. **19**(6): p. 2351-2358.
11. Liu, Y., et al., *Preparation and characterization of chitosan-gelatin/glutaraldehyde scaffolds.* Journal of Macromolecular Science, Part B, 2013. **53**(2).
12. Yu, Y., et al., *Synthesis and Characterization of N -maleyl Chitosan-Cross-Linked Poly(acrylamide)/Montmorillonite Nanocomposite Hydrogels.* Polymer-Plastics Technology and Engineering, 2011. **50**(5): p. 525-529.
13. Peppas, N.A. and A.R. Khare, *Preparation, structure and diffusional behavior of hydrogels in controlled release.* Advanced Drug Delivery Reviews, 1993. **11**(1-2): p. 1-35.
14. Ratner, B.D., A.S. Hoffman, and J.D. Andrade, *Synthetic Hydrogels for Biomedical Applications*. Hydrogels for Medical and Related Applications. Vol. 31. 1976, Washington :. 1-36.
15. Hoare, T.R. and D.S. Kohane, *Hydrogels in drug delivery: Progress and challenges.* Polymer, 2008. **49**(8): p. 1993-2007.
16. Williams, D.F., *The Williams Dictionary of Biomaterials*. 1999: Liverpool University Press. 343.
17. Esposito, E., R. Cortesi, and C. Nastruzzi, *Gelatin microspheres: influence of preparation parameters and thermal treatment on chemico-physical and biopharmaceutical properties.* Biomaterials, 1996. **17**(20): p. 2009-2020.
18. Nagahama, H., et al., *Preparation, characterization, bioactive and cell attachment studies of α-chitin/gelatin composite membranes.* International Journal of Biological Macromolecules, 2009. **44**(4): p. 333-337.
19. Moghimi, S.M., A.C. Hunter, and J.C. Murray, *Long-Circulating and Target-Specific Nanoparticles: Theory to Practice.* Pharmacological Reviews, 2001. **53**(2): p. 283-318.
20. Vinogradov, S.V., T.K. Bronich, and A.V. Kabanov, *Nanosized cationic hydrogels for drug delivery: preparation, properties and interactions with cells.* Advanced Drug Delivery Reviews, 2002. **54**(1): p. 135-147.
21. Park, J.S., et al., *Poly(N-isopropylacrylamide-co-acrylic acid) nanogels for tracing and delivering genes to human mesenchymal stem cells.* Biomaterials, 2013. **34**(34): p. 8819-8834.

22. Georgopoulou, A., et al., *Chitosan/gelatin scaffolds support bone regeneration.* Official Journal of the European Society for Biomaterials, 2018. **29**(5): p. 1-13.
23. Van Der Linden, H.J., et al., *Stimulus-sensitive hydrogels and their applications in chemical (micro)analysis.* The Analyst, 2003. **128**(4): p. 325-331.
24. Ciobanu, B.C., et al., *Modulated release from liposomes entrapped in chitosan/gelatin hydrogels.* Materials Science & Engineering C, 2014. **43**: p. 383-391.
25. Amsden, B., *Solute diffusion within hydrogels. Mechanisms and models.* Macromolecules, 1998. **31**(23): p. 8382-8395.
26. Canal, T. and N.A. Peppas, *Correlation between mesh size and equilibrium degree of swelling of polymeric networks.* Journal of biomedical materials research, 1989. **23**(10): p. 1183-1193.
27. Mason, M.N., et al., *Predicting Controlled-Release Behavior of Degradable PLA- b -PEG- b -PLA Hydrogels.* Macromolecules, 2001. **34**(13): p. 4630-4635.
28. Bajpai, S.K. and S. Singh, *Analysis of swelling behavior of poly(methacrylamide-co-methacrylic acid) hydrogels and effect of synthesis conditions on water uptake.* Reactive and Functional Polymers, 2006. **66**(4): p. 431-440.
29. Wu, J., Z.-G. Su, and G.-H. Ma, *A thermo- and pH-sensitive hydrogel composed of quaternized chitosan/glycerophosphate.* International Journal of Pharmaceutics, 2006. **315**(1-2): p. 1-11.
30. Thakur, V.K. and M.K. Thakur, *Hydrogels : Recent Advances*. 2018, Singapore: Singapore: Springer.
31. Ross-Murphy, S.B., *Rheological characterization of polymer gels and networks.* Polymer Gels and Networks, 1994. **2**(3-4): p. 229-237.
32. Parhi, R., *Cross-Linked Hydrogel for Pharmaceutical Applications: A Review.* Advanced Pharmaceutical Bulletin, 2017. **7**(4): p. 515-530.
33. Berger, J., et al., *Structure and interactions in covalently and ionically crosslinked chitosan hydrogels for biomedical applications.* European Journal of Pharmaceutics and Biopharmaceutics, 2004. **57**(1): p. 19-34.
34. Elliott, J.E., et al., *Structure and swelling of poly(acrylic acid) hydrogels: effect of pH, ionic strength, and dilution on the crosslinked polymer structure.* Polymer, 2004. **45**(5): p. 1503-1510.
35. Baldino, L., et al., *Complete glutaraldehyde elimination during chitosan hydrogel drying by SC-CO2 processing.* The Journal of Supercritical Fluids, 2015. **103**: p. 70-76.
36. Oikawa, H. and H. Nakanishi, *A light scattering study on gelatin gels chemically crosslinked in solution.* Polymer, 1993. **34**(16): p. 3358-3361.
37. Monteiro, O.A.C. and C. Airoldi, *Some studies of crosslinking chitosan–glutaraldehyde interaction in a homogeneous system.* International Journal of Biological Macromolecules, 1999. **26**(2-3): p. 119-128.
38. Robert O. Beauchamp, M.B.G.S.C., Timothy R. Fennell, David O. Clarke, Kevin T. Morgan & Frank W. Karl, *A Critical Review of the Toxicology of Glutaraldehyde.* Critical Reviews in Toxicology, 1992. **22**(3-4): p. 143-174.
39. Boucard, N., C. Viton, and A. Domard, *New aspects of the formation of physical hydrogels of chitosan in a hydroalcoholic medium.* Biomacromolecules, 2005. **6**(6): p. 3227.
40. Adrus, N. and M. Ulbricht, *Rheological studies on PNIPAAm hydrogel synthesis via in situ polymerization and on resulting viscoelastic properties.(Report).* Reactive and Functional Polymers, 2013. **73**(1): p. 141.
41. Pelton, R., *Temperature-sensitive aqueous microgels.* Advances in Colloid and Interface Science, 2000. **85**(1): p. 1-33.
42. Farooqi, Z.H., et al., *Stability of poly(N-isopropylacrylamide-co-acrylic acid) polymer microgels under various conditions of temperature, pH and salt concentration.* Arabian Journal of Chemistry, 2017. **10**(3): p. 329-335.
43. Varga, I., et al., *Effect of cross-link density on the internal structure of poly(N-isopropylacrylamide) microgels.* Journal of Physical Chemistry B, 2001. **105**(38): p. 9071-9076.

44. Si, T., et al., *Effect of acrylic acid weight percentage on the pore size in poly(N-Isopropyl acrylamide- co-acrylic acid) microspheres.* Reactive and Functional Polymers, 2011. **71**(7): p. 728-735.
45. Wisniewska, M.A., J.G. Seland, and W. Wang, *Determining the scaling of gel mesh size with changing crosslinker concentration using dynamic swelling, rheometry, and PGSE NMR spectroscopy.* Journal of Applied Polymer Science, 2018. **135**(45): p. n/a-n/a.
46. Niţă, L., et al., *In situ monitoring the sol–gel transition for polyacrylamide gel.* Rheologica Acta, 2007. **46**(5): p. 595-600.
47. Okay, O., *Macroporous copolymer networks.* Progress in Polymer Science, 2000. **25**(6): p. 711-779.
48. Righetti, P.G., C. Gelfi, and A.B. Bosisio, *Polymerization kinetics of polyacrylamide gels. III. Effect of catalysts.* ELECTROPHORESIS, 1981. **2**(5-6): p. 291-295.
49. Kiene, K., et al., *Self-assembling chitosan hydrogel: A drug-delivery device enabling the sustained release of proteins.* Journal of Applied Polymer Science, 2018. **135**(1): p. n/a-n/a.
50. Bhattarai, N., J. Gunn, and M. Zhang, *Chitosan-based hydrogels for controlled, localized drug delivery.* Advanced Drug Delivery Reviews, 2010. **62**(1): p. 83-99.
51. Rinaudo, M., G. Pavlov, and J. Desbrières, *Influence of acetic acid concentration on the solubilization of chitosan.* Polymer, 1999. **40**(25): p. 7029-7032.
52. Muzzarelli, R.A.A., *Chitin*. First Edition ed. 1977: Pergamon Press.
53. Costa, C.N., et al., *Viscometric study of chitosan solutions in acetic acid/sodium acetate and acetic acid/sodium chloride.* Carbohydrate Polymers, 2015. **133**: p. 245-250.
54. J. Berger, M.R., J.M. Mayer, O. Felt, R. Gurny, *Structure and interactions in chitosan hydrogels formed by complexation*

or aggregation for biomedical applications. European Journal of Pharmaceutics and Biopharmaceutics, 2004. **57**(1): p. 35-52.
55. Yang, Y., et al., *The controlling biodegradation of chitosan fibers by N-acetylation in vitro and in vivo.* Official Journal of the European Society for Biomaterials, 2007. **18**(11): p. 2117-2121.
56. Jumaa, M., F.H. Furkert, and B.W. Müller, *A new lipid emulsion formulation with high antimicrobial efficacy using chitosan.* European Journal of Pharmaceutics and Biopharmaceutics, 2002. **53**(1): p. 115-123.
57. van Den Broek, L.A.M., et al., *Chitosan films and blends for packaging material.* Carbohydrate Polymers, 2015. **116**: p. 237-242.
58. Kean, T. and M. Thanou, *Biodegradation, biodistribution and toxicity of chitosan.* Advanced Drug Delivery Reviews, 2010. **62**(1): p. 3-11.
59. Ueno, H., T. Mori, and T. Fujinaga, *Topical formulations and wound healing applications of chitosan.* Advanced Drug Delivery Reviews, 2001. **52**(2): p. 105-115.
60. Tseng, H.J., et al., *Characterization of chitosan–gelatin scaffolds for dermal tissue engineering.* Journal of Tissue Engineering and Regenerative Medicine, 2013. **7**(1): p. 20-31.
61. Argüelles-Monal, W., et al., *Rheological study of the chitosan/glutaraldehyde chemical gel system.* Polymer Gels and Networks, 1998. **6**(6): p. 429-440.
62. Gómez-Guillén, M.C., et al., *Functional and bioactive properties of collagen and gelatin from alternative sources: A review.* Food Hydrocolloids, 2011. **25**(8): p. 1813-1827.
63. Djabourov, M. and P. Papon, *Influence of thermal treatments on the structure and stability of gelatin gels.* Polymer, 1983. **24**(5): p. 537-542.
64. Carvalho, W. and M. Djabourov, *Physical gelation under shear for gelatin gels.* An International Journal of Rheology, 1997. **36**(6): p. 591-609.
65. Derkach, S.R., N.G. Voron'ko, and N.I. Sokolan, *The rheology of hydrogels based on chitosan–gelatin (bio)polyelectrolyte complexes.* Journal of Dispersion Science and Technology, 2017. **38**(10): p. 1427-1434.
66. Kawahara, J.-I., et al., *The structure of glutaraldehyde in aqueous solution determined by ultraviolet absorption and light scattering.* Analytical Biochemistry, 1992. **201**(1): p. 94-98.

67. Harrington, J.C. and E.R. Morris, *Conformational ordering and gelation of gelatin in mixtures with soluble polysaccharides.* Food Hydrocolloids, 2009. **23**(2): p. 327-336.
68. Peter, M., et al., *Preparation and characterization of chitosan–gelatin/nanohydroxyapatite composite scaffolds for tissue engineering applications.* Carbohydrate Polymers, 2010. **80**(3): p. 687-694.
69. Badawy, M.E.I., et al., *Preparation and Characterization of Biopolymers Chitosan/Alginate/Gelatin Gel Spheres Crosslinked by Glutaraldehyde.* Journal of Macromolecular Science, Part B, 2017. **56**(6): p. 359-372.
70. Cui, L., et al., *Preparation and characterization of IPN hydrogels composed of chitosan and gelatin cross-linked by genipin.* Carbohydrate Polymers, 2014. **99**: p. 31-38.
71. Rokhade, A.P., S.A. Patil, and T.M. Aminabhavi, *Synthesis and characterization of semi-interpenetrating polymer network microspheres of acrylamide grafted dextran and chitosan for controlled release of acyclovir.* Carbohydrate Polymers, 2007. **67**(4): p. 605-613.
72. Paar, A. *Basics of rheology*. [cited 2019 09.05.19]; Available from: https://wiki.anton-paar.com/en/basics-of-rheology/.
73. Carrington, S. *Rheology explained part 2 - oscillation & viscoelasticity*. [Webinar] 2011 08.10.2018 [cited 2019 08.08]; Available from: https://www.malvernpanalytical.com/en/learn/events-and-training/webinars/W110526RheologyExplainedPart2.
74. Paar, A. *Amplitude sweeps*. [cited 2019 30.05]; Available from: https://wiki.anton-paar.com/en/amplitude-sweeps/.
75. Paar, A. *Frequency sweeps*. [cited 2019 30.05]; Available from: https://wiki.anton-paar.com/en/frequency-sweeps/.
76. Flory, P.J., *Principles of polymer chemistry*. 1953, Ithaca: Cornell University Press.
77. Nie, J., B. Du, and W. Oppermann, *Swelling, Elasticity, and Spatial Inhomogeneity of Poly(N -isopropylacrylamide)/Clay Nanocomposite Hydrogels*. 2005. p. 5729-5736.
78. Nie, J., B. Du, and W. Oppermann, *Influence of Formation Conditions on Spatial Inhomogeneities in Poly(N -isopropylacrylamide) Hydrogels (Book review).* Macromolecules, 2004. **37**(17): p. 6558-6564.
79. Calvet, D., J.Y. Wong, and S. Giasson, *Rheological Monitoring of Polyacrylamide Gelation: Importance of Cross-Link Density and Temperature*. 2004: Washington, D.C. :. p. 7762-7771.
80. Haggerty, L., et al., *Diffusion of polymers through polyacrylamide gels.* Polymer, 1988. **29**(6): p. 1058-1063.
81. Stejskal, E.O. and J.E. Tanner, *Spin Diffusion Measurements: Spin Echoes in the Presence of a Time-Dependent Field Gradient.* The Journal of Chemical Physics, 1965. **42**(1): p. 288-292.
82. Adrjan, B., et al., *Comparison of electrochemical- and nuclear magnetic resonance spectroscopy methods for determination of diffusion coefficients in gel environment.* Electrochimica Acta, 2014. **144**: p. 228-234.
83. Wallace, M., D.J. Adams, and J.A. Iggo, *Analysis of the mesh size in a supramolecular hydrogel by PFG-NMR spectroscopy.* Soft Matter, 2013. **9**(22): p. 5483-5491.
84. Stilbs, P., *Fourier transform pulsed-gradient spin-echo studies of molecular diffusion.* Progress in Nuclear Magnetic Resonance Spectroscopy, 1987. **19**(1): p. 1-45.
85. Li, B., et al., *PGSE NMR studies of water states of hydrogel P(Am–NaA.* Journal of Applied Polymer Science, 2000. **77**(2): p. 424-427.
86. Peter Atkins, J.d.P., *Atkins' Physical Chemistry*. 10 ed. 2014: Oxford University Press.
87. Kestin, J., et al., *Viscosity of light and heavy water and their mixtures*. 1985: Amsterdam :. p. 38-58.
88. Paar, A. *How to measure viscosity*. [cited 2019 26.05]; Available from: https://wiki.anton-paar.com/en/how-to-measure-viscosity/.
89. Mao, J.S., et al., *Structure and properties of bilayer chitosan–gelatin scaffolds.* Biomaterials, 2003. **24**(6): p. 1067-1074.

90. Gao, X., et al., *pH- and thermo-responsive poly(N -isopropylacrylamide- co -acrylic acid derivative) copolymers and hydrogels with LCST dependent on pH and alkyl side groups.* J. Mater. Chem. B, 2013. **1**(41): p. 5578-5587.
91. Pavlov, G., et al., *Hydrodynamic properties of cyclodextrin molecules in dilute solutions.* with Biophysics Letters, 2010. **39**(3): p. 371-379.
92. Lin, C.-C. and A.T. Metters, *Hydrogels in controlled release formulations: Network design and mathematical modeling.* Advanced Drug Delivery Reviews, 2006. **58**(12-13): p. 1379-1408.